8-AQ

EXPERIMENTAL AND THEORETICAL STUDY OF MUD PULSE PROPAGATION

A Thesis

Submitted to the Graduate Faculty of the
Louisiana State University and
Agricultural and Mechanical College
in partial fulfillment of the
requirements for the degree of
Master of Science

in
The Department of Petroleum Engineering

by
Joseph Alan Carter
B.S., Mississippi State University, 1983
May, 1986

Carter, Joseph Alan, B.S. Mississippi State University, 1983
Master of Sience, Spring Commencement, 1986
Major: Petroleum Engineering
<u>Experimental and Theoretical Study of Mud Pulse Propagation</u>
Thesis directed by Dr. Robert Desbrandes
Pages in Thesis, 63. Words in Abstract, 266.

Mud pressure pulse propagation is directly related to the data transmission rate in Measurement While Drilling (MWD). Recently MWD techniques have evolved into a sophisticated drilling monitoring and formation evaluation system. What was traditionally a directional package now includes bottom hole drilling parameter measurement devices and logging sensors. Recording of weight on bit, torque, pressure, temperature, resistivity and radioactivity can be made. Such information are invaluable for drilling efficiency, safety and formation evaluation. Great advances have been achieved in the technology of recording information but little progress has been made in increasing the rate of data transmission. The experimental results presented in this paper are in good agreement with the theoretical calculations showing that the theory for pulse propagation can be used for most types of muds and conditions.

The velocity and attenuation of pressure pulses have been measured with a 9,460 ft, 4 1/2" drill pipe loop. The loop is equipped with fast pressure gages located at

various distances. A tape recorder and a wave analyser were used for a thorough and accurate study of the propagation. The mud pulser used was a fluidic pulser providing a perfect control of the pulse frequency up to 25 Hz. After testing the equipment, water, water base and oil base muds of various characteristics were used. The experimental results supported the theory derived by White and Watters on pressure pulse velocity and also the theory of Lamb on attenuation. At 25 Hz, in oil base mud, signal attenuation of −17 dB (0.14 of initial value) could be detected at the opposite end of the loop.

Basic data are provided in this work for designing more efficient MWD systems.

AKNOWLEDGEMENT

Sincere thanks are extended to Dr. Robert Desbrandes, Professor of Petroleum Engineering at the Louisiana State University, under the supervision and guidance of whom this work was completed. Appreciation is also extended to Dr. Ted Bourgoyne, Professor of Petroleum Engineering at the Louisiana State University, who's advice and guidance during the early stages of this research proved to be invaluable. The author would also like to thank Mr. James Sykora, Mr. Allen Kelly, and Mr. Mark Chauvin, coordinators at the L.S.U. Blowout Control School and Research Center. It is with their assistance and cooperation that helped make this project a success. Suggestions and collaboration by the remainder of the faculty is also greatly appreciated.

This project was funded by the Minerals Management Service, a division of the Department of the Interior of the United States Government.

TABLE OF CONTENTS

Page

ACKNOWLEDGEMENT....................................ii

TABLE OF CONTENTS..................................iii

LIST OF TABLES..................................... v

LIST OF FIGURES....................................vi

ABSTRACT... viii

CHAPTER

I. INTRODUCTION....................................1

II. VELOCITY AND ATTENUATION THEORY...................6

2.1 Velocity Theory...............................6

2.2 Attenuation Theory............................9

III. EXPERIMENTAL MODEL...............................13

3.1 Experimental system...........................13

3.2 Recording and Analyzing Equipment.............24

3.3 Operational Procedure.........................29

IV. EXPERIMENTAL RESULTS.............................36

4.1 Calibration Check.............................36

4.2 Water Results.................................38

4.3 Water-Base Mud Results........................45

4.4 Oil-Base Mud Results..........................51

4.5 Discussion of Results.........................56

V. CONCLUSIONS AND RECOMENDATIONS....................59

5.1 Conclusions....................................59

5.2 Recomendations.................................60

REFERENCES...61

VITA...63

LIST OF TABLES

Table		Page
1	ICP Transducer Specifacations..............	18
2	ICP Power Supply Specifacations............	19
3	Table of Measured Properties of the Fluids used in the Experiment..............	33

LIST OF FIGURES

FIGURE		PAGE
1	Typical Bottom Hole Assembly for MWD	2
2	Three Types of Mud Pulsers in Present Use	4
3	Experimental Loop	14
4	Pump Frequency and Piston Action	15
5	Cross-section of Transducer	20
6	Schematic of Internal Components of the Pressure Measuring Devices	20
7	Diaghram of the Mounting of the Transducer	21
8	A Vortex Valve and Parts	23
9	Flow Through a Vortex Valve	25
10	A Picture of the Pulser	26
11	Pump Noise Spectrum	31
12	A Sine Wave and Its Spectrum	34
13	Calibration Results	37
14	A 2 Hertz Frequency from Water Runs	39
15	Plot of Wave Velocity in Water	40
16	Fourier Transform of Figure 14	42
17	Intensity vs. Distance in Water (3 Hz)	43
18	Attenuation vs. Frequency in Water	44
19	Wave Velcocity in Waterbase Mud	47

20 Attenuation vs. Frequency (Mud #1).........48

21 Attenuation vs. Frequency (Mud #2).........49

22 Attenuation vs. Frequency (Mud #3).........50

23 A 13 Hertz Signal Generated by the Pulser.....................................53

24 Wave Velocity in Oil Base Mud..............54

25 Amplitude vs. Distance in Oil Base Mud at 13 Hertz.............................55

26 Attenuation vs. Frequency in Oil Base Mud (Mud #4)..............................57

ABSTRACT

Mud pressure pulse propagation is directly related to the data transmission rate in Measurement While Drilling (MWD). Recently MWD techniques have evolved into a sophisticated drilling monitoring and formation evaluation system. What was traditionally a directional package now includes bottom hole drilling parameter measurement devices and logging sensors. Recording of weight on bit, torque, pressure, temperature, resistivity and radioactivity can be made. Such information are invaluable for drilling efficiency, safety and formation evaluation. Great advances have been achieved in the technology of recording information but little progress has been made in increasing the rate of data transmission. The experimental results presented in this paper are in good agreement with the theoretical calculations showing that the theory for pulse propagation can be used for most types of muds and conditions.

The velocity and attenuation of pressure pulses have been measured with a 9,460 ft, 4 1/2" drill pipe loop. The loop is equipped with fast pressure gages located at various distances. A tape recorder and a wave analyser were used for a thorough and accurate study of the propa-

gation. The mud pulser used was a fluidic pulser providing a perfect control of the pulse frequency up to 25 Hz. After testing the equipment, water, water base and oil base muds of various characteristics were used. The experimental results supported the theory derived by White and Watters on pressure pulse velocity and also the theory of Lamb on attenuation. At 25 Hz, in oil base mud, signal attenuation of −17 dB (0.14 of initial value) could be detected at the opposite end of the loop.

Basic data are provided in this work for designing more efficient MWD systems.

CHAPTER 1

INTRODUCTION

Directional drilling is becoming more important as drilling spreads to deep water platforms and other confined drilling locations. With the large number of directional holes originating from a central location, there comes a necessity to know the precise path of the well. This is important for several reasons such as reaching the bottom hole target, drilling safety, formation evaluation, and drilling optimization. Conventionaly, well bore surveys have been done by wireline operations. Due to the costly time associated with wireline trips, it has been found economically beneficial to survey some wells (mainly offshore) by a means know as Measurement While Drilling (MWD). This system incorporates sensors in the drill string for measuring downhole parameters and transmitting them uphole through the drill pipe in the form of coded pressure pulses. Figure (1) shows a typical bottom hole assembly for MWD [1]. There are presently three types of mud pulsers used for data transmission [2]. They are:

1) Negative Pulse. Pulses are generated by venting the drilling fluid from the drill string into the annulus (Figure 2a).

2) Positive Pulse. Positive pulses are created by a mechanical valve which restricts

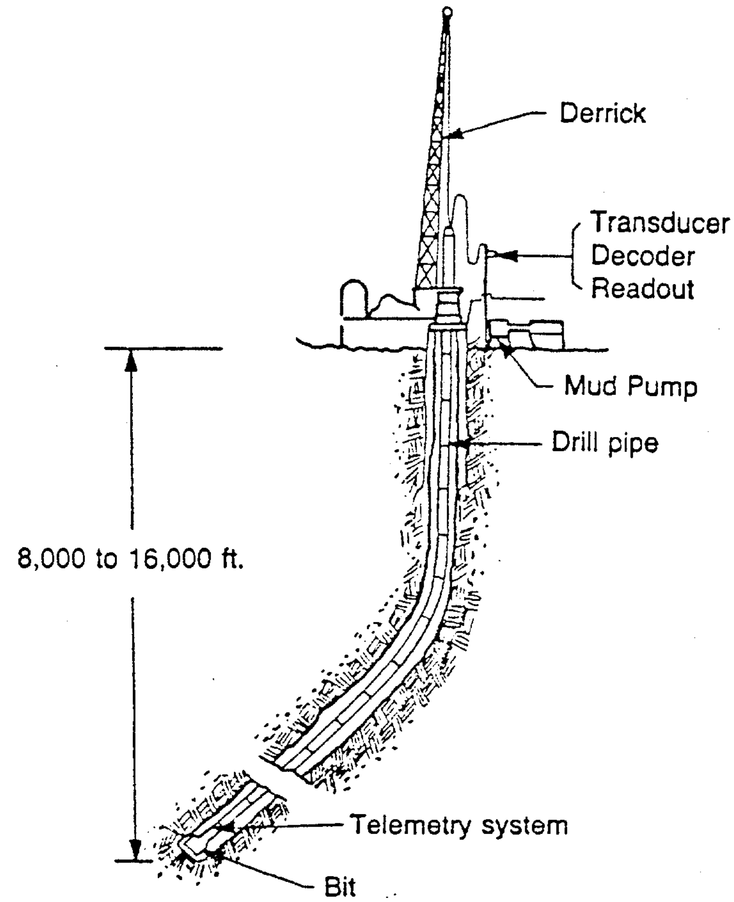

Figure 1. Typical Bottom Hole Assembly of a Measurement While Drilling System.

flow through the pipe (Figure2b).

3) Continuous Wave. A pulse frequency is generated by a rotating turbine in the drill string. The data is encoded in phase shifts of this frequency (Figure 2c).

Although Measurement While Drilling is considered a common method of obtaining directional parameters on offshore rigs, this method of well telemetry has become much more than just a directional package. Since the introduction of MWD for commercial use in 1978 by Teleco Oilfield Services Ltd. [1], several innovations in technology have evolved. What was merely a directional package is now capable of several functions. MWD companies now offer logging sensors such as a gamma ray and resistivity. There are also other bottom hole parameters available such as weight on bit, torque, temperature, and pressure. Information such as this is desirable to optomize drilling procedures and more important for safety of personnel.

However, with the increase in bottom hole data there is also an increase in the total time it takes to transmit this data to the surface. This is due to the necessity to constantly update all information concerning the formation. Some MWD tools are programmed for an update every minute on bottom hole activity. The present transmission rates are not well suited for repeatedly trans-

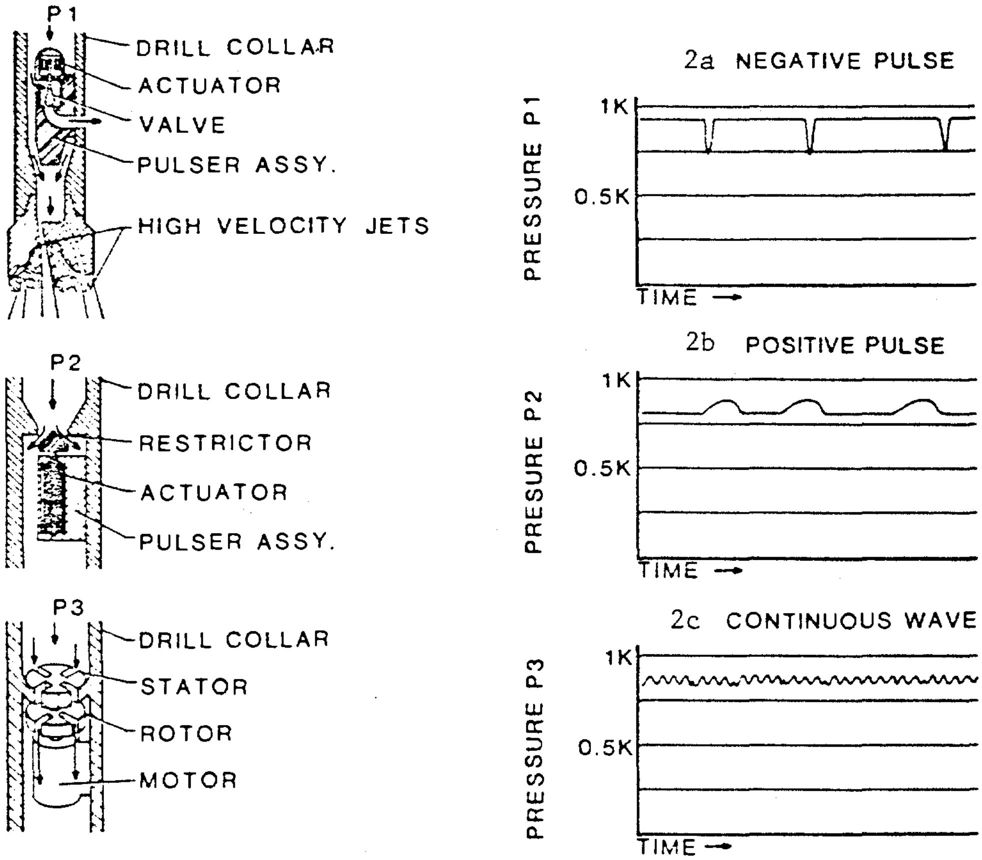

Figure 2. Three Types of Mud Pulsers Presently Being used for Pressure Pulse Transmission.

mitting such large volumes of data. This inconvenience can be alleviated in two areas. First by altering the coding system of the pressure pulses, and second by increasing the pulse rate itself. It is the purpose of this research to determine if it is possible to receive signals on the surface at relatively high frequencies.

In order to accomplish this, the first objective is to establish a method to compute the sonic velocity in the drill pipe. Two approaches will be considered, each will be compared to experimentally obtained data. As a second objective of this research, hydrodynamic equations derived by Lamb [6] will be verified by experimental data. These equations were derived to compute the attenuation of pressure pulses in pipes as a function of viscosity and frequency. It is necessary to establish a relationship between frequency and pulse attenuation to determine an optimum transmission rate.

CHAPTER 2

VELOCITY AND ATTENUATION THEORY

2.1 Velocity Theory

The attenuation of a pulse in a tube is a function of several factors. The first factor examined is the velocity in which the pulse travels. It is necessary to determine the pulse velocity in order to compute the attenuation. Therefore a reliable equation must be found to calculate wave velocities. This particular value is dependent upon the size and type of tube and also the characteristics of the fluid through which it propagates. There has been more than one approach to the calculation of wave velocities in pipes. This paper has evaluated two equations for use in drill pipe. The first of these is equation (1) derived by Watters [3].

$$V = 144\rho g_c \left(\frac{1}{B} + \frac{1}{M}\right)^{-1/2} \quad (1)$$

with longitudinal restraint

$$\frac{1}{M} = \frac{4b^2(1-\lambda^2) + 2(1+\lambda)(a^2-b^2)}{E(a^2-b^2)} \quad (2)$$

where

v = Velocity (Ft/sec)

B = Bulk Modulus of Elasticity of the Fluid (psi)

E = Young's Modulus of Elasticity (psi)

a = Outer Diameter of Pipe (in.)

b = Internal Diameter of Pipe (in.)

g_c = Units Conversion (32.17)

λ = Poisson's Ratio

ρ = Density (lb/ft^3)

M = Pipe Modulus (psi)

The pipe modulus "M" is dependent on the pipe properties and also on how the pipe is anchored. Watters has derived a pipe modulus for three different types of restraint. In case "A" above there is no longitudinal strain allowed. This is a characteristic of the system. In this experiment the pipe is buried and is expected to be restrained from longitudinal expansion by soil friction. There are however, equations for computing the pipe modulus for other situations. For instance consider the case where the drill string is in the borehole and on bottom, one might choose to use the equation for case "B" where:

$$\frac{1}{M} = \frac{4b^2(5/4-\lambda) + 2(1+\lambda)(a^2+b^2)}{E(a^2-b^2)} \tag{3}$$

This equation allows for stress and strain both laterally and longitudinally. This would most likely be the case for all instances associated with drilling conditions. Watters also developed an expression for pipes with functioning expansion joints throughout their length. This configuration is not likely to be encountered in the drilling phase of the industry but will be included in the text for the benefit of the reader. This type of stress and strain condition will be referred to as case "C" and the pipe modulus is represented as

$$\frac{1}{M} = \frac{4b^2 + 2(1+\lambda)(a^2-b^2)}{E(a^2-b^2)} \tag{4}$$

Equations 2, 3, and 4 are derived so that the pipe modulus for thick and thin walled pipes can be computed and plugged into equation (1).

The second equation studied in the experiment was derived by White [4]. The two equations are very similar in that they both were derived from the same approach. Each author chose to include the elasticity of the pipe, both longitudinal and lateral displacements. Though the equations appear different in the text of White and Watters, the only difference in the two equations is the way the pipe modulus is computed. Therefore through algebraic rearrangement, the equation by White can be represented as another means of calculating the pipe modulus and plugging into equation (1) to get the wave velocity. The equation by White,

$$\frac{1}{M} = \frac{2[(1+\lambda)(a^2+b^2) - 2\lambda b^2]}{E(a^2-b^2)} \tag{5}$$

includes some work done by Lamb on radial displacement due to a pressure on the interior of a thick-walled tube. The expressions presented by White on the subject are for thick-walled pipe and low frequency waves.

Despite the two different equations the velocity calculations from the equations differed by only about 2 ft/sec for the fluids used in this experiment. This can probably be attributed to the rigidity of the drill pipe. This margin of closeness may lead one to choose either equation in the case of drill pipe. However, for the computations of this experiment the equation by Watters will be used to represent a case "A" or longitudinal restraint. It will be a goal of this work to obtain experimental data to support the theory of these equations.

2.2 Attenuation Theory

Once the wave velocity is established one can study the aspects of pulse attenuation. There have been extensive studies performed on water hammer effects in pipes. This has led to some research on short single pulses in pipes also. Equation (6) represents part of the research performed by Rouleau [5] on single pulses.

$$\frac{P_{(x,t)}-\bar{P}}{P_o} = \begin{cases} 0 \\ e^{-To}\ \mathrm{erfc}[1/2To(T-To)^{-1/2}] \\ e^{-To}\ (\mathrm{erfc}[1/2To(T-To)^{-1/2}] - \mathrm{erfc}[1/2To(T-To-\Delta T)^{-1/2}]) \end{cases} \tag{6}$$

for
$$T < T_o$$
$$T_o \leqq T < T_o + \Delta T$$
$$T \geqq T_o + \Delta T$$

where

$$T = \frac{\nu}{b^2}t \quad (7) \qquad T = \frac{\nu x}{b^2 V} \quad (8) \qquad T = \frac{\nu}{b^2}t_o \quad (9)$$

$P_{(x,t)}$ = Fluid Pressure (lb/ft^2)

$\overline{P}$ = Reservoir Pressure of Experiment (lb/ft^2)

P_o = Magnitude of Pressure Pulse (lb/ft^2)

T = Non-Dimensional Time

T_o = Non-Dimensional Time Delay

ΔT = Non-Dimensional Duration Time of Pulse

Equation (6) will predict the amplitude of a single pulse traveling through a static fluid column at any distance x from the origin. Although this can give some insight to the dissipation of a pressure pulse over a distance, it is not applicable to Measurement While Drilling systems because in nearly all cases of MWD the data is transmitted through a series or burst of pulses in a dynamic environment. For this reason the effect of frequency must be taken into account on pulse attenuation.

Some classical work of this nature has been performed by Lamb[6]. Lamb has derived that the change in pulse amplitude traveling along a tube is given by

$$P_{(x)} = P_o e^{-x/L} \tag{10}$$

and

$$L = \frac{bV}{2} \frac{2}{\nu\omega} \tag{11}$$

where

b = Inside Diameter of Pipe (ft)

V = Pulse Velocity (ft/sec)

ν = Kinematic Viscosity of Fluid (ft^2/sec)

ω = Angular Frequency (rad/sec)

P_x = Pulse Amplitude at Distance x (psi)

P_o = Original Pulse Amplitude (psi)

L = Distance in Which Amplitude Falls to 1/e of its Original Value (ft)

The angular frequency ω can be computed by

$$\omega = 2\pi f \tag{12}$$

where f is the pulse frequency in Hertz. The velocity computations have been discussed previously in the paper. The one problem which must be resolved now is that the equation calls for the kinematic viscosity and not the traditional plastic viscosity which is normally encountered in the Bingham plastic model of the oil industry. This is accomplished by substituting the absolute viscosity with the plastic viscosity and then converting to the kinematic viscosity. The conversion can be done by using equation (13) from Marks Mechanical Engineering Handbook [7].

$$\nu = 2.09\ 10^{-5}\ \frac{\mu g_c}{\rho} \qquad (13)$$

ν = Kinematic Viscosity (ft^2/sec)

μ = Absolute (Plastic) Viscosity (cp)

g_c = Units Conversion

ρ = Density (lb/ft^3)

The attenuation equations were derived long ago by Lamb, however, there is little experimental data to verify the accuracy of the equations. The attenuation theory behind the derivations is based on Newtonian fluids. It will be one of the goals of this work to perform experiments with Newtonian and Non-Newtonian (Bingham Plastic) fluids and evaluate the performance of Lamb's attenuation equations. In the case of the Bingham Plastic fluids, the plastic viscosity will be substituted for the absolute viscosity and then calculations will be carried through as in the Newtonian fluid. It is expected that while the mud is in the drill pipe and in turbulent flow, the shear rate will remain at such a value that the fluid will behave in a near Newtonian fashion.

CHAPTER 3

EXPERIMENTAL MODEL

3.1 Experimental System

A mud loop has been built to conduct the tests at the Louisiana State University Blowout School and Research Center. The conduit consists of 9,460 feet of 4.5 inch, 20 pound per foot, API drill pipe. The pipe forms two connecting loops and was buried 5 feet underground with the mid-section and both ends rising to the surface. There are concrete manholes at selected intervals to allow access to the drill pipe. Figure (3) illustrates an overall view of the experimental set up. This grade of drill pipe has a 3.64 inch internal diameter and a capacity of 1.2871 barrels per 100 linear feet.

The pump connected to the loop was a Halliburton HT-400 triplex pump. The pump was equiped with 4 inch liners and has an 8 inch stroke length. This coupled with an output efficiency of 99% delivered a pump factor of approximately 1.28 gallons per stroke [8].

Due to the characteristics of a pump of this nature, it was necessary to dampen the pulsation caused by the pistons of the pump. Figure (4a) and (4b) illustrate the pressure surges generated by a duplex and triplex pump respectively [9]. It can be seen that the pressure is not steady but actually a continuous fluctuation of pres-

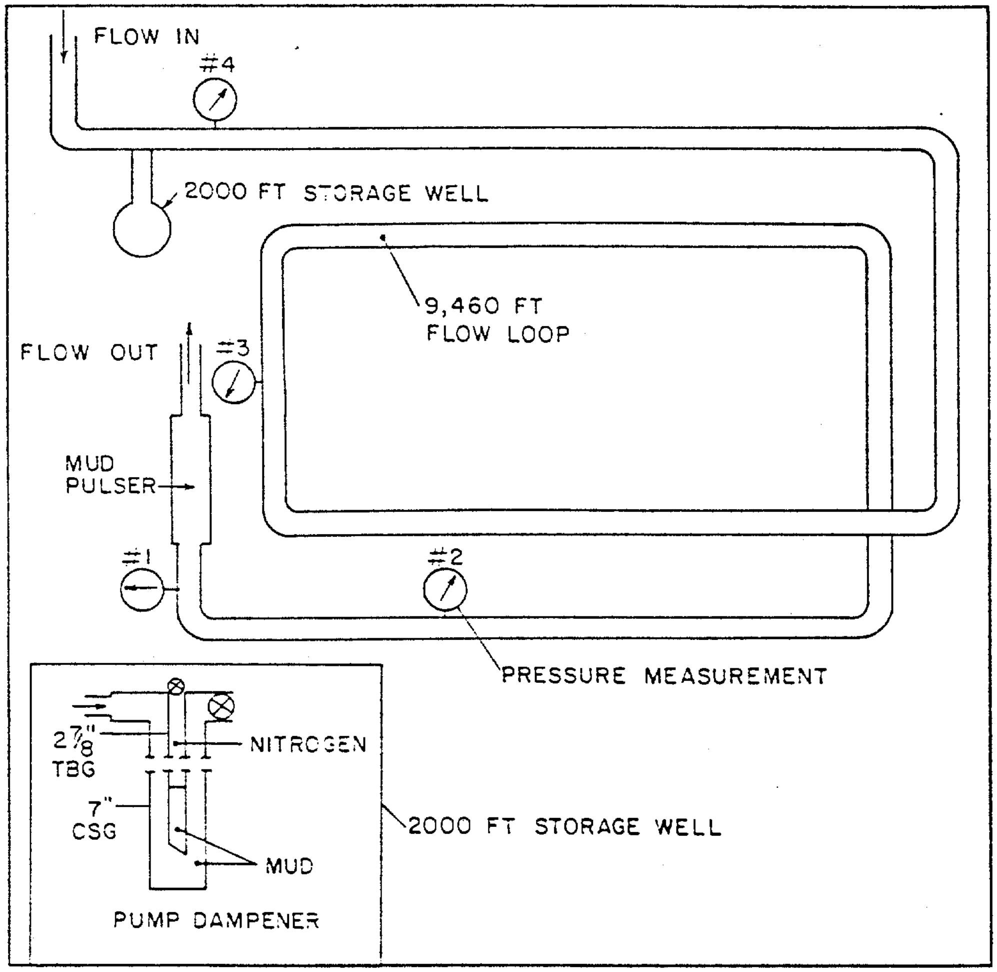

Figure 3. Flow Loop Built at the L.S.U. Research Center for Conducting Experiments.

DUPLEX DOUBLE-ACTING PUMP

Total Flowrate Variation: 45.6%

Average Flow

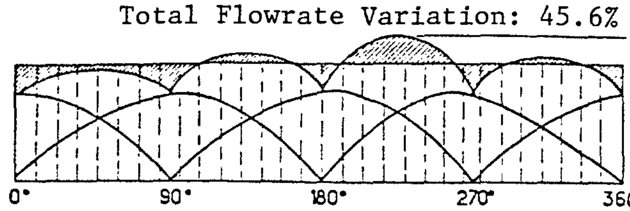

Max. Flow:+24.1%

Min. Flow:-21.5%

Rotation Angle 0

TRIPLEX SINGLE-ACTING PUMP

Total Flowrate Variation: 23%

Average Flow

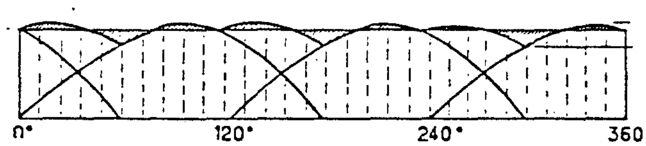

Max.Flow:+6.1%
Min.Flow:-16%

Rotation Angle 0

Figure 4. Diaghram of Duplex and Triplex Pump Pressure Performance.

sure peaking as each pump piston strikes the fluid. This fluctuation can be smoothed out considerably by interconnecting the outlet of the pump with a pocket or chamber containing a compressible fluid to act as a shock absorber. Two dampeners were used in this experiment. First a small air filled dampener was mounted directly on the pump. This particular dampener was non-chargeable and totally inadequate for experimental purposes. To reinforce the dampening, a nearby 2,000 feet well was connected 6 feet ahead of the inlet end of the drill loop. The well was equiped with an open-ended tubing. The tubing was charged with approximately 150 pounds per square inch of nitrogen. This displaced 320 feet of mud from the tubing and served as a cushion for the pump noise. Although this provided a significant amount of dampening, the proper equipment would have been several 5 to 10 gallon bladder type pulsation dampeners. This has proven successful in experiments performed by Mobil Research and Development Corporation [10].

The pressure measurement devices consist of hydraulic pressure sensors to measure pump pressure and piezoelectric quartz transducers to monitor pressure pulses. The transducers are constructed specifically for measuring dynamic pressures. Figure (5) gives a cross-sectional view of a transducer. The high impedance voltage signal produced by the quartz element is fed across the input of a built-in constant current follower amplifier which converts the signal to a low impedance voltage. This voltage is low enough to be fed directly into recording equipment.

The transducers are powered by AC or DC mode line power units. The power units supply excitation to transducers and also couples self-amplifying transducers to readout instrumentation. Figure (7) gives a schematic of the internal components of the transducer and its power supply. In the coupling process the power supply eliminates DC power bias from the output by means of a coupling capacitor or level shifter of the floating DC power supply type. The power supply generates a constant-current excitation which is adjustable from 2 mA to 20 mA. The current is factory set at about 4 mA. The current may be increased to drive longer cables or to provide more output voltage. The factory setting was sufficient to drive the 300 feet cables used in this experiment, however, due to problems of humidity seeping into the transducer connections, the current supply was stepped up to 15 mA output. The transducers are rated for 10,000 psi working pressure and 1000 psi dynamic pressure measurement. Table (1) and Table (2) give other specifications of the transducers and power supplies respectively. From Table (1) it is shown that the transducers have a rise time of 3 micro-seconds which is

Range (5V Output)	1,000 psi
Useful Overrange (10V Output)	2,000 psi
Maximum Pressure	10,000 psi
Resolution	.005 psi
Sensitivity	5 mV/psi
Resonant Frequency	200 KHz
Rise Time	3 μS
Discharge Time	100 S
Low Frequency Response (-5%)	.5 Hz
Polarity	Positive
Output Impedence	100 Ω
Output Bias	9 to 12 V
Temperature Range	-100 to +275°F
Flash Temperature	3000°F
Vibration Shock	2,000/20,000 g
Excitation (Constant Current)	2 to 20 mA

Table 1. Specifacations of PCB Model 121A02 Quartz Transducers.

Excitation, Constant	2 to 20 mA
Current (Set at 15)	24V DC
Voltage Gain (Non-Inverting)	1.00
Coupling Capacitor	10 μF
Coupling Time Constant	
(AC Mode)	10 S
Bias Elimination Range	
(DC Mode)	4.5 to 6.2 V
Frequency Response	
(±5%, DC Mode)	DC to 200 KHz
Frequency Response	
(±5%, AC Mode)	.05 to 200 KHz
Output Current	10 ±mA
Output Impedence	50 Ω
Noise (pk-to-pk)	600 μV

Table 2. Specifacations of PCB Model 484M57 Constant Current Power Supply.

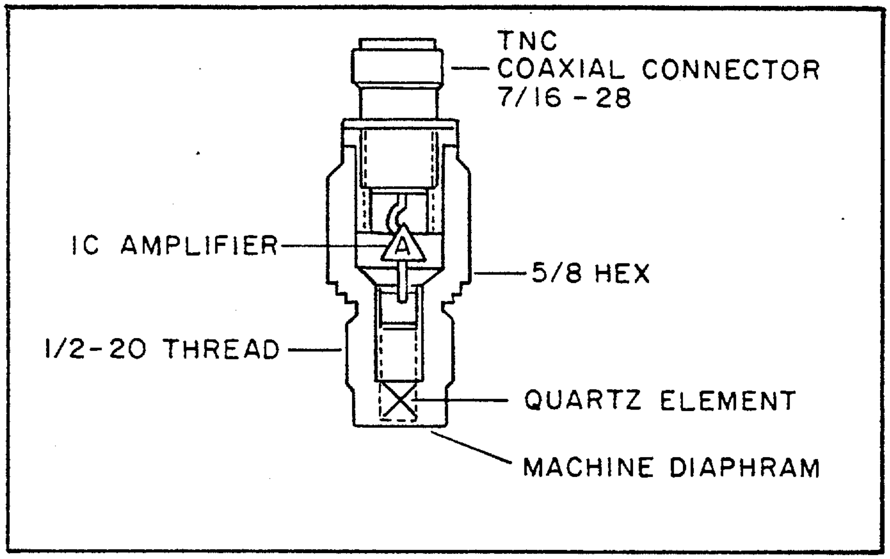

Figure 5. Cross-Sectional View of a Transducer used for Dynamic Pressure Measurement.

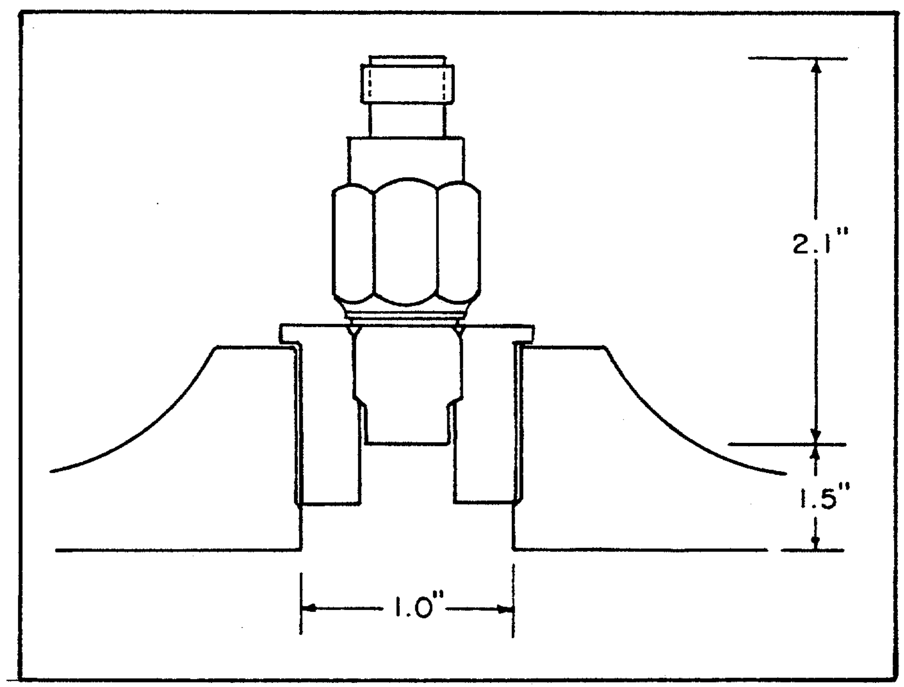

Figure 6. Mounting Technique of the Transducers.

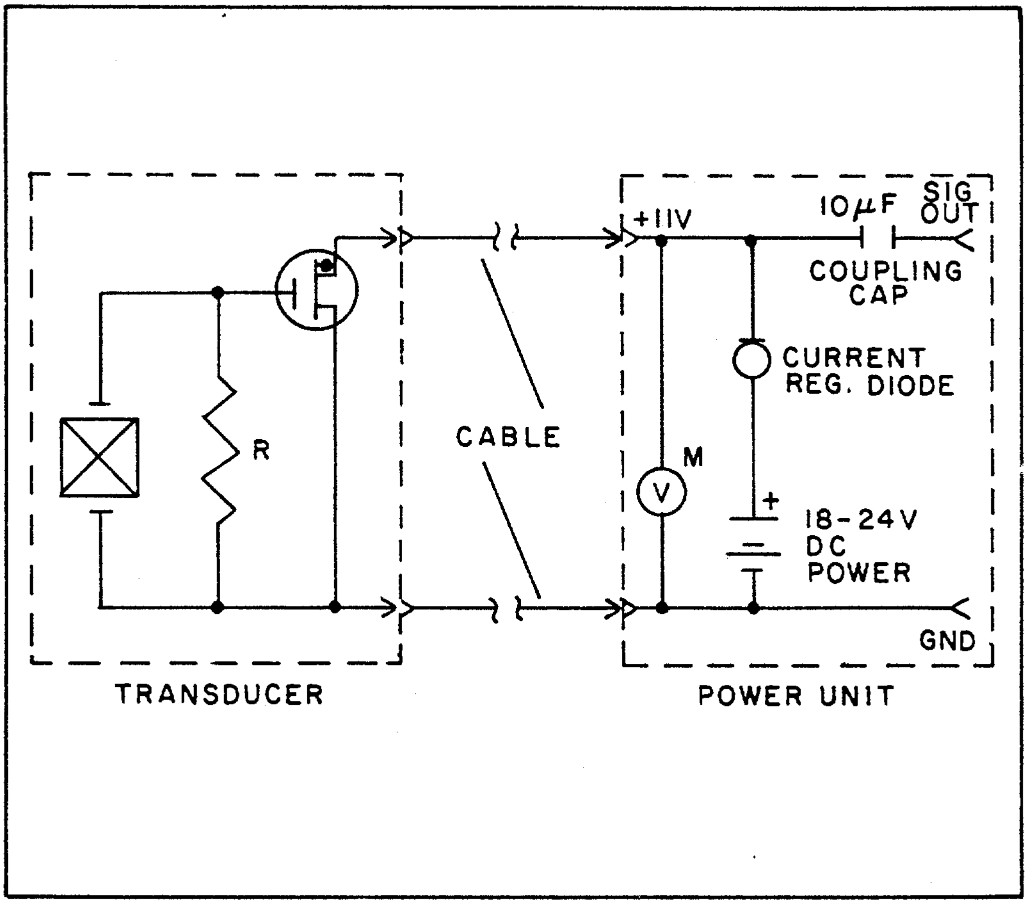

Figure 7. Schematic of the Internal Components of the Transducers and Power Supplies.

sufficient to distinguish and measure pulses at relativly high frequencies [11].

The transducers are located in four taps along the drill pipe. They were mounted carefully to avoid damage and as close as possible to the fluid medium to insure little or no air entrapment (figure 6). The transducers were located as follows:

#1 located 25 feet from the pulser

#2 located 280 feet from the pulser

#3 located 4730 feet from the pulser

#4 located 9460 feet from the pulser

The pump was connected approximately 100 feet from the last transducer. Discharge from the pulser was returned through a manifold and return line consisting of 300 feet of 2 inch heavy gauge line pipe.

The tool used to generate a pulse was a prototype developed by Harry Diamond Laboratories in Washington, D. C. The pulser is unique in its design. It consists of fluidic type valves which employ centrifugal forces to create a vortex flow which in turn causes an increased pressure drop in the high loss mode. A vortex valve is shown in figure (8). Figure (9) shows the two types of flow through such a valve. It can be seen that the fluid flows easily through the valve with little pressure loss before the vortex is induced (figure 9a). When the tab is actuated to create the vortex (figure 9b), a pressure

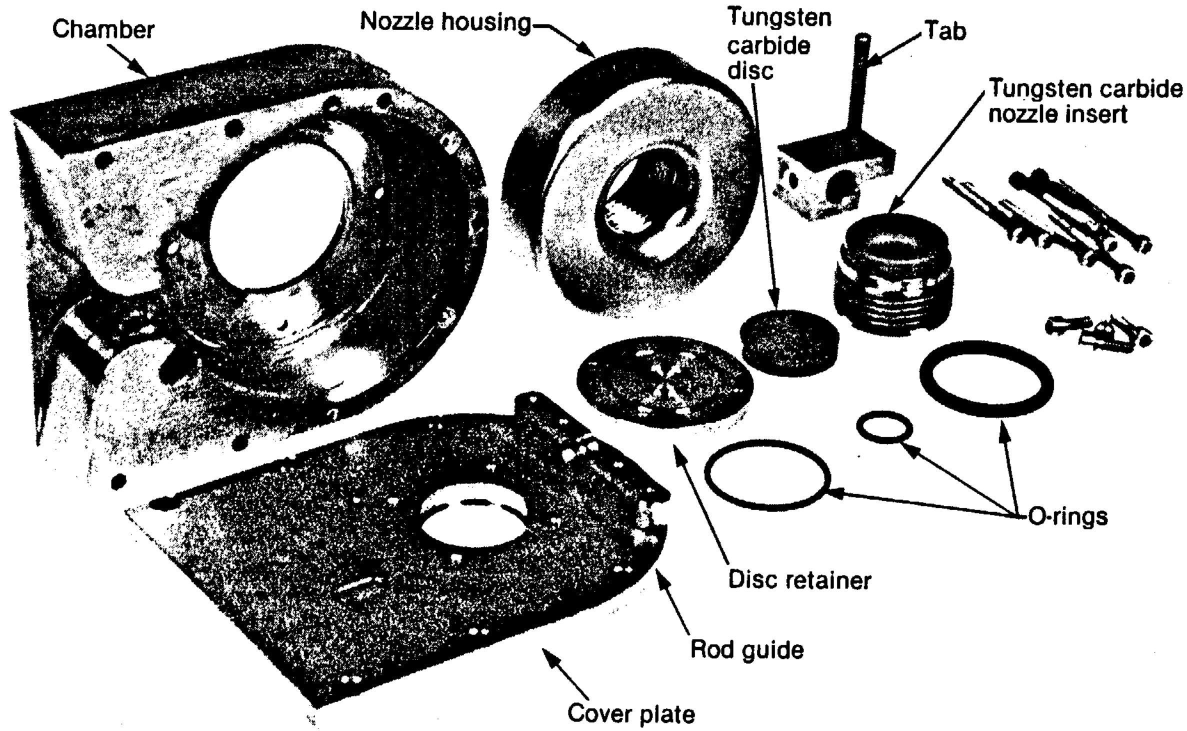

Figure 8. Tab Actuated Vortex Valve Components.

surge is created by the centrifugal forces acting around the chamber and through the outlet [12].

The tab is mechanically driven by a small fast acting solenoid. The solenoid is isolated from the drilling fluid and operates through a bellows. The pressure between the solenoid and the drilling fluid is equalized through a rubber diaphram. This keeps the solenoid free of mud solids and prevents it from working against needless pressure differentials.

The vortex valves can be connected in parallel to adapt to high flow rates or simply blocked off or port areas reduced to handle lower flow rates. Figure (10) shows the entire pulser with four vortex valves in parallel. In this experiment two vortex valves were used. Only two were necessary due to a limited flow rate of 200 gallons per minute [13]. The pressure drop through the tool in the open or unactivated position was around 120 psi compared with approximately 95 psi with 4 vortex valves. This is representative of the versatility of the tool without high gains in frictional pressure loss.

3.2 Recording and Analyzing Equipment

Data was collected and stored on magnetic analog tape. The recorder was equipped to handle five tracks plus an edge track. Channels one through four contained the output from the transducers. The fifth channel on the tape recorded the signal from the signal generator

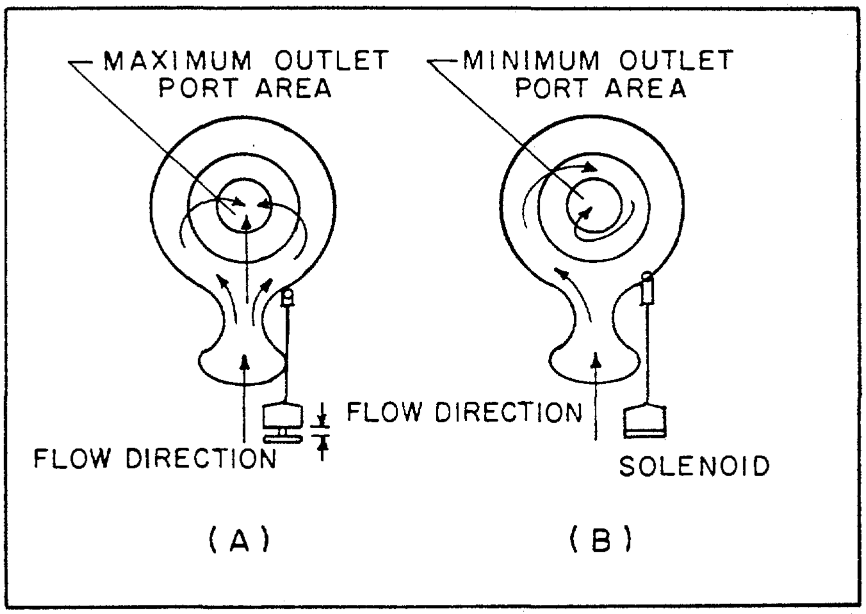

Figure 9. Flow Through a Vortex Valve. (A) Low Pressure Loss Mode. (B) High Pressure Loss Mode.

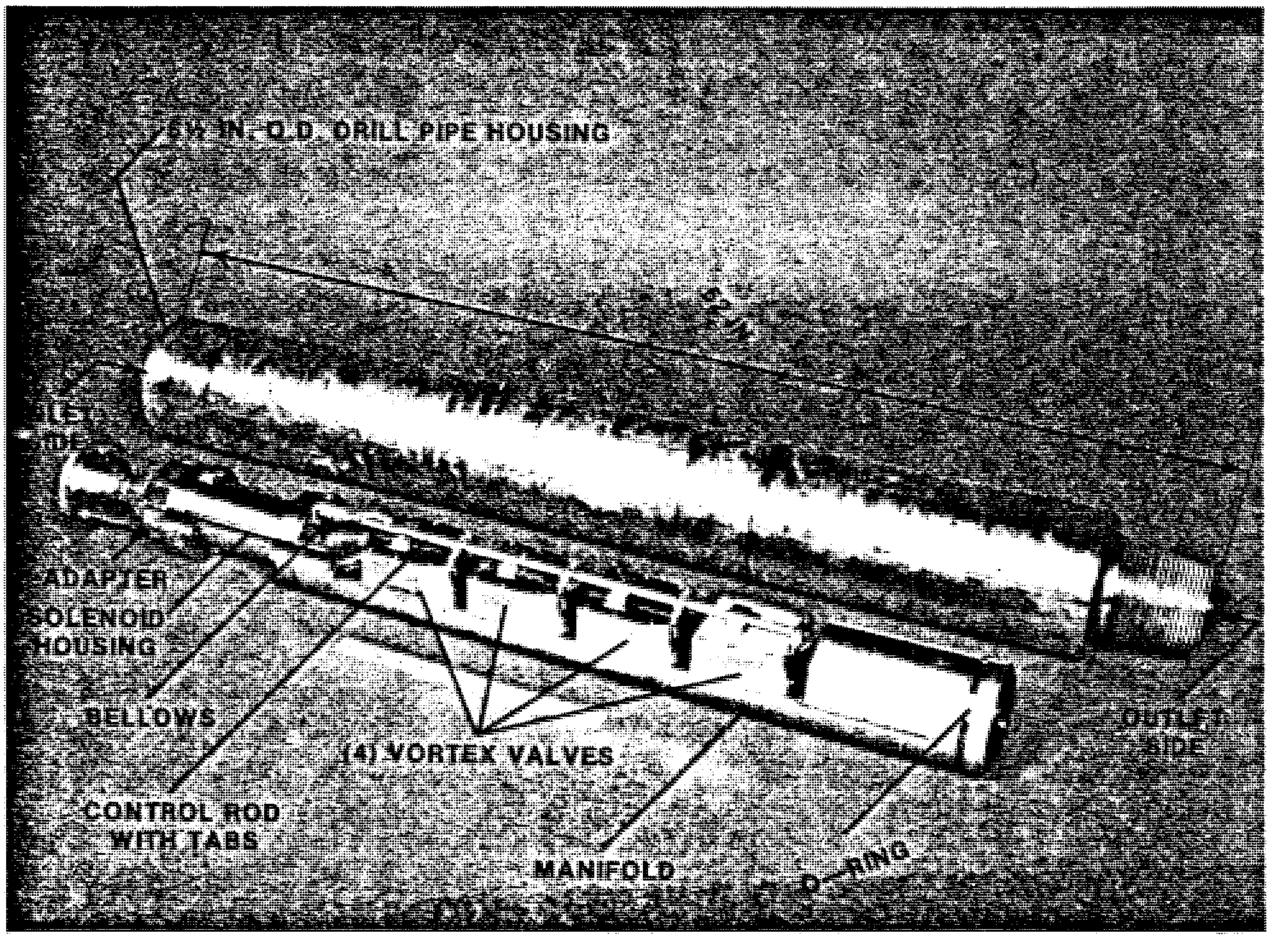

Figure 10. Fluidic Mud Pulser with Four Tab Actuated Vortex Valves.

which produced a square wave input to the pulser. The outside or edge track was used as an audio track to record a vocal account of various stages of the experiment.

The instrument used to analyze the data was a Wavetek Cross Channel Spectrum analyzer. This instrument had several convenient and necessary functions. It was capable of processing data at intervals and averaging data before displaying the result. The analyzer was also capable of working in communication with small computers, calculators, and printers. This provided a convenient hard copy of data for analysis and future reference. The most favorable function of the spectrum analyzer was its pre-programmed menus. The most interesting of these is its ability to perform Fast Fourier Transforms [14].

Fourier analysis is commonly found in engineering practices. Many complex periodic waves are mixtures of harmonic waves of several frequencies. This leads to a mathematical analysis originating with what is known as Fourier's theorem. This theorem allows any periodic function to be analyzed in terms of sines and cosines. Consider the periodic function f(t), Fourier's theorem states that this function can be written as

$$f_{(t)} = A_o + \sum_n (A_n \text{Sin}\, \omega_n t + B_n \text{Cos}\, \omega_n t) \tag{14}$$

where

$$\omega_n = n\,\frac{2\pi}{T} \tag{15}$$

n = Harmonic Number

ω = Frequency

T = Period

This is known as the Fourier Series of f(t). The relative values of A_n and B_n are related to the waveform. The value $A_n^2 + B_n^2$ is proportional to the intensity of the nth harmonic component of the function [15]. As part of the Fourier analysis the components A_o, B_n, and A_n, can be determined by the so called Euler formulas [15]:

$$A_o = \frac{1}{2\pi}\int_{-\pi}^{\pi} f_{(t)}\, dt \tag{16}$$

$$A_n = \frac{1}{\pi}\int_{-\pi}^{\pi} f_{(t)} \text{Cos } nt\, dt \tag{17}$$

$$B_n = \frac{1}{\pi}\int_{-\pi}^{\pi} f_{(t)} \text{Sin } nt\, dt \tag{18}$$

The Fourier transform is an integral expression for a Fourier series applied to an infinately long signal. The fundamental wave and its harmonics are seperated by infinitesimal increments. Fourier transform techniques are used to express a time function as a continuous function of frequency and also to synthesize a function expressed in terms of amplitude versus frequency into the function of time to which it corresponds. The mathematical expression of Fourier transform comes in two parts, one for the frequency spectrum F(ω) in terms of the time function f(t) and the other for the time function in terms of the frequency spectrum. The frequency function F(ω) can be obtained by the integral [17]

$$F_{(\omega)} = \int_{-\infty}^{\infty} f_{(t)} \text{Cos } 2\pi\omega t \; dt - i\int_{-\infty}^{\infty} f_{(t)} \text{Sin } 2\pi\omega t \; dt \qquad (19)$$

Similarly the transmorm f(t) can be expressed by the integral

$$f_{(t)} = \int_{-\infty}^{\infty} F_{(\omega)} \text{Cos } 2\pi\omega t \; d\omega + i\int_{-\infty}^{\infty} F_{(\omega)} \text{Sin } 2\pi\omega t \; d\omega \qquad (20)$$

Needless to say, it can be a difficult task to perform such mathematics without the aid of a computer. The Wavetek Spectrum Analyzer uses a network of processors to perform Fast Fourier Transform Computations. The Fast Fourier Transform is merely a digitized exponential method of performing the Fourier transform previously discussed [18].

3.3 Operational Procedure

A systematic program of steps were performed and repeated throughout the course of the experiment. The procedure began with a calibration check of the transducers. All transducers were mounted together and made to undergo a series of pulses to ensure that each device had been calibrated to the same output. Following the initial calibration check the transducers were spread out along the drill pipe. Once the transducers had been mounted in their proper place, a steady flow of approximately 200 gallons per minute (GPM) was established. To run at 200 GPM the pump must operate at 160 to 165 strokes per minute. At this speed the pump pistons generate a frequency of approximately 8.25 Hz. Therefore, to obtain as pure of a pulse as possible, frequencies of 1, 2, 3, 5, 10, 13, and 20 Hz were chosen as the most adequate points to be analyzed. Figure (11) is a recording of the pump noise and its spectrum. It can be seen that the selected frequencies allow the experiments to be conducted with the least amount of interference from the pump pulsation. Upon completion of a set of given experiments, the transducers were again mounted together and their calibrations checked. This was found necessary from experience, to make certain that the data collected was accurate and of good quality.

The experiment consisted of running fluids most likely encountered in drilling operations. The fluids used were fresh water, water-base mud, and oil-base mud. The

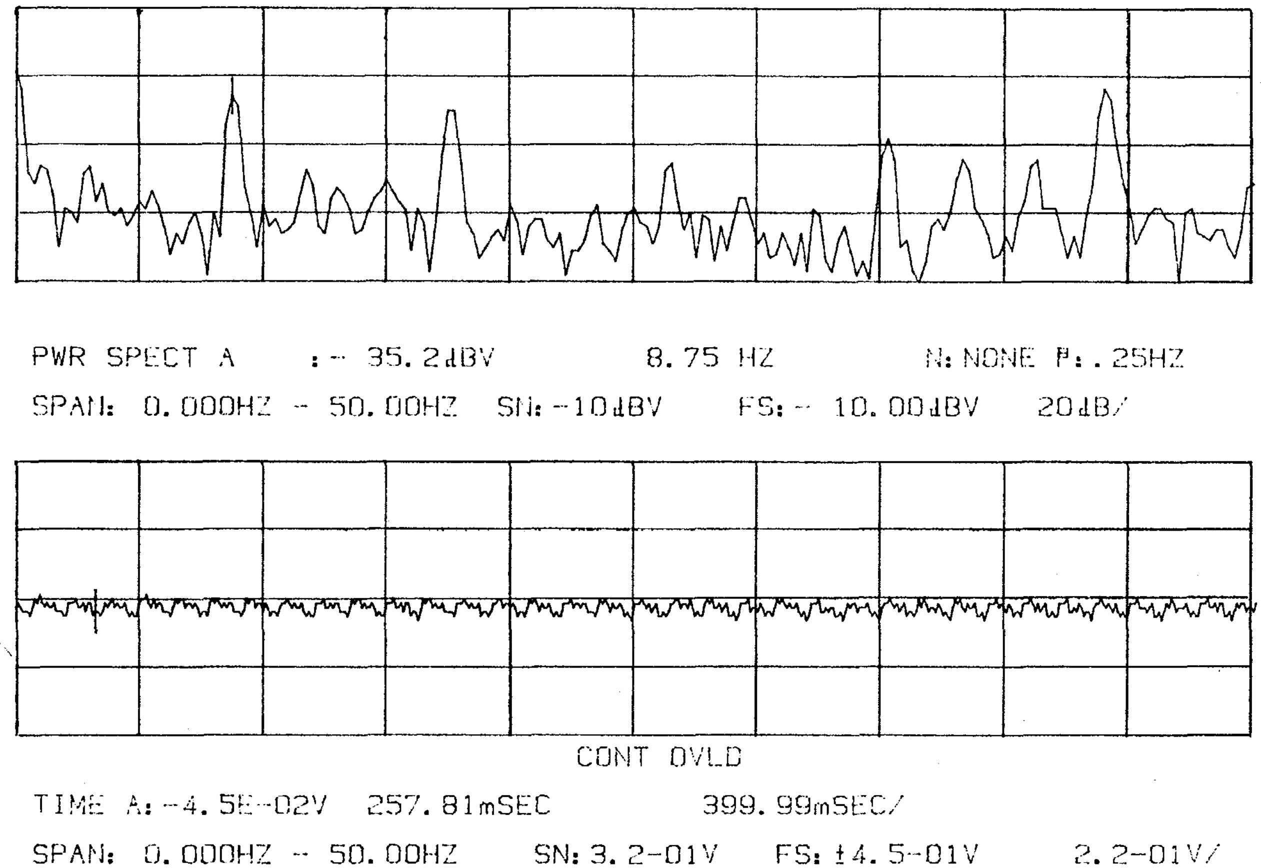

Figure 11. Recording of Pump Noise and its Fourier Transform.

physical properties of the muds were altered repeatedly in order to analyze their effect on attenuation. Table (3) states the fluids used in the experiment.

Once the data had been collected and stored on tape, it was then possible to reproduce the data and examine carefully the velocity and attenuation phenomena. The most promising method of interpretation seemed to be the Fourier spectrum of the curves generated. The reason for this is that there are so many harmonic waves that propagate through the fluid from the pulser as well as the pump. In this method the time domain is transformed to a frequency domain through Fourier analysis. The result is a graph of fundamental and harmonic frequencies versus intensity. Figure 12a is representative of the Fourier transform of a 10 Hz sine wave (12b). This allows an easy isolation of the pulse and provides a more accurate measurement of its magnitude. As mentioned earlier, rather than solving any complicated mathematical problems, a Wavetek Spectrum Analyzer was used to perform the transform.

In the Fourier transform the intensity is proportional to the magnitude of that particular frequency. In the case of the Wavetek, the intensity is measured in decibels (db). It was found useful to establish a relationship between the intensity and actual voltage amplitude of the signal. Through a series of signal

PROPERTIES	WATER	WATER-BASE MUD			OIL-BASE MUD
		Mud #1	Mud #2	Mud #3	Mud #4
Density (lb/gal)	8.3	8.9	8.9	8.9	8.5
Funnel Viscosity (sec)	27	41	47	57	49
Plastic Viscosity (cp)	1	14	20	26	20
Yield Point (lb/100 ft)	---	4	7	9	4
Fan Readings	*	*	*	*	*
600 RPM	---	32	47	64	44
300 RPM	---	18	27	38	24
200 RPM	---	14	20	28	16
100 RPM	---	7	12	16	9

Table 3. Measured Properties of Various fluids used in the Experiment.

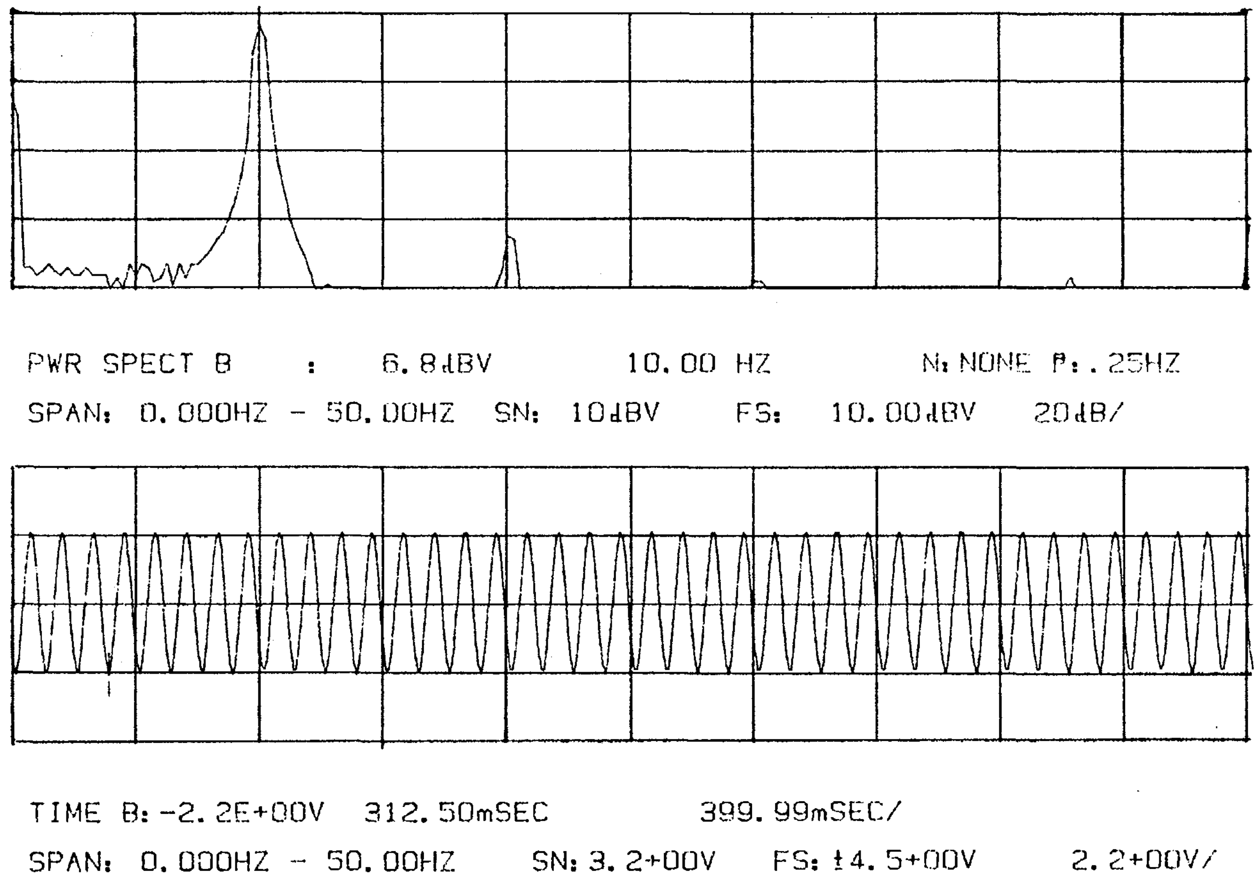

Figure 12. A Pure 10 Hertz Sine Wave From a Signal Generator. (A) The Frequency Domain of the Sine Wave. (B) The Time Domain of the Sine Wave.

inputs, as in figure (12), equation (20) was found to give a quick conversion.

$$Vpp = 2 \times 10^{db/20} \tag{21}$$

where

Vpp = Peak to Peak Amplitude of Wave (volts)

db = Value of Fourier Transform (decibels)

With a known transducer output of 5 millivolts per psi, this equation makes it simple to translate signal strengths into more familiar units of psi.

CHAPTER 4

EXPERIMENTAL RESULTS

4.1 Calibration Check

The experiment began with an equipment check. The transducers were mounted on a manifold and tested for accuracy and to assure sufficient response. The manifold was packed with grease to prevent air from being trapped and in turn projecting false or misleading calibration data. During the initial stages of the experiment some moisture problems were encountered with the transducers. The quartz transducers used in the tests contained a built-in amplifier. Any dampness in or around the amplifier caused a shorting out or change in resistance within the transducer. With the cooperation of the manufacturer this problem was alleviated by sealing 6 feet of coaxial cable to the connector of the transducer. This seemed to work well and allowed the experiment to continue without interruptions.

Once environmental problems were conquered the sensitivity of the transducers was checked. The results indicated that the transducers were very closely calibrated to the same output. Figure (13) is representative of the calibration results. The maximum deviation by a transducer was about 3 tenths of a dB. Therefore, it was decided that 5 tenths of a dB would be an acceptable margin for transducer accuracy.

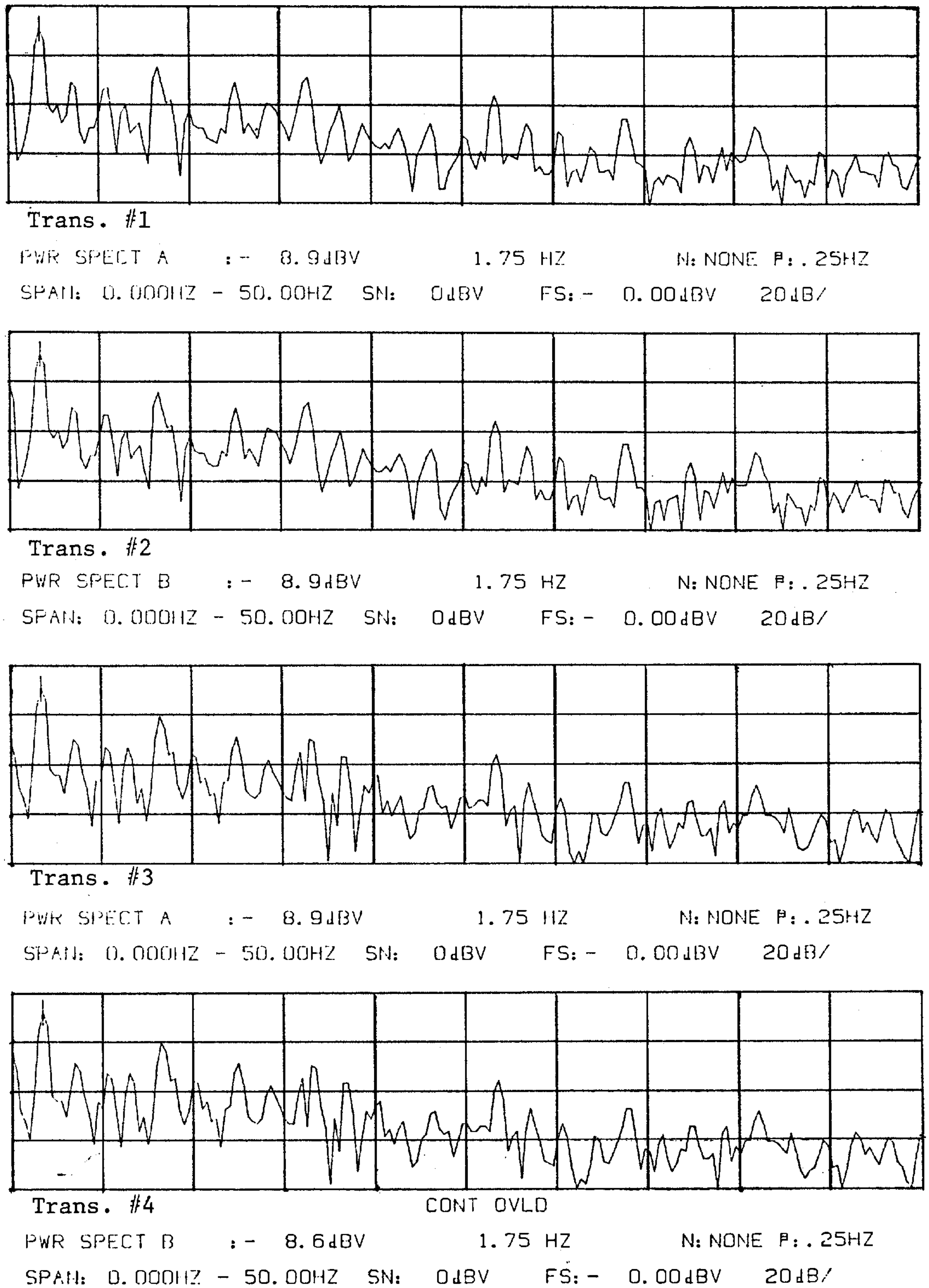

Figure 13. Typical Results of Calibration Runs on Transducers Before and Following a Set of Experiments.

4.2 Water Results

The velocity and attenuation tests were first conducted with water. Figure (14) is an example of a 2 hertz wave generated by the pulser. The attenuation is difficult to see here because there is very little attenuation at this distance and frequency when water is the fluid medium. Although Figure (14) was not applicable to the attenuation calculations it was very useful in calculating travel times. By producing an overlay of the signal from the first transducer, it was possible to fit the pulses over the signals produced by the other transducers. Then by measuring the time difference from the first transducer and the others the wave velocity was computed. The experimentally determined wave velocity in the water medium was about 4900-4920 feet per second.

This corresponds well to the theoretical value of 4910 feet per second which was computed using the equation derived by Walters [3]. Figure (15) is a plot of the experimental data and the theoretical value for wave velocity in water. The equation by White [4] also produces a comparable value of 4909 feet per second. However, the equation by Watters describes the present system more accurately and produces a value closest to the measured velocity.

The attenuation measurements were made using the Fourier Transform of the pulse generated. Figure (16) is

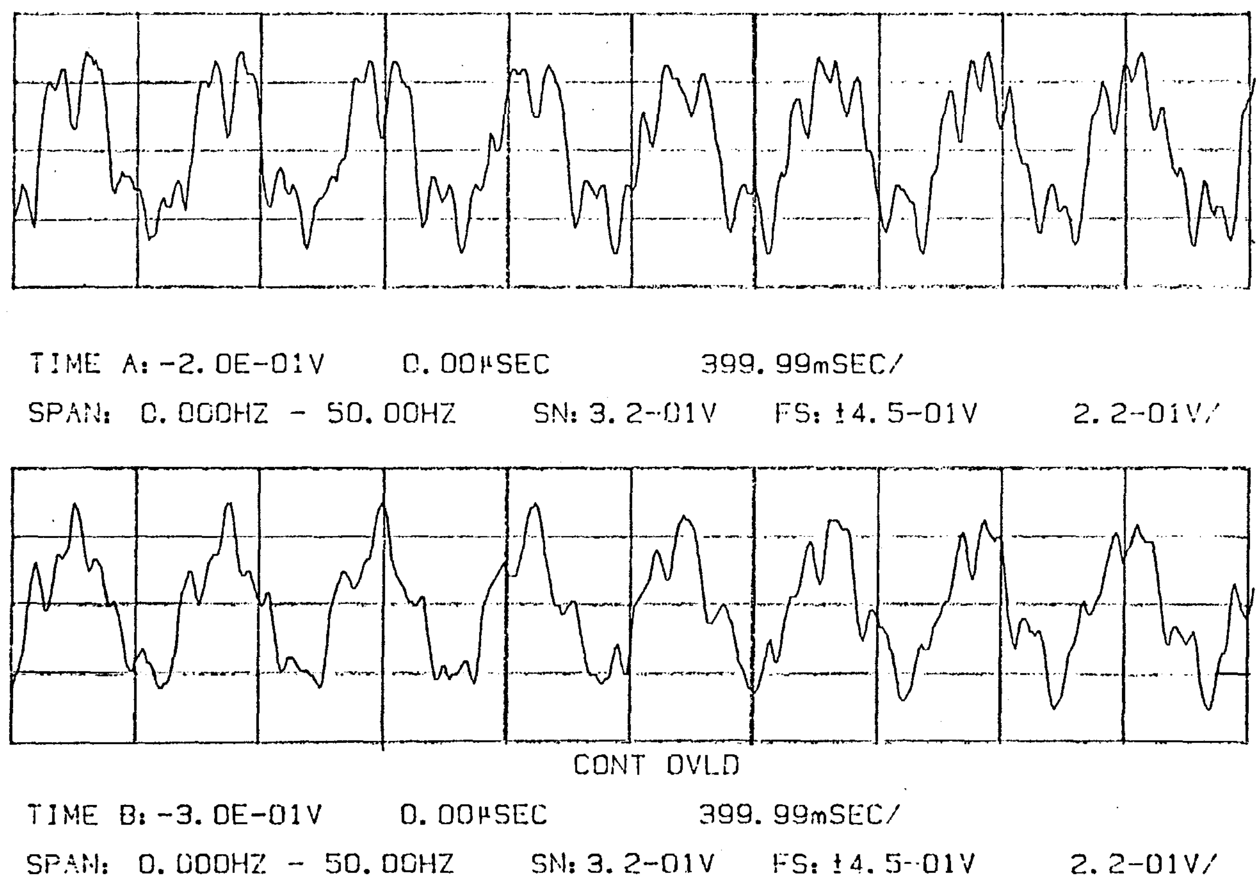

Figure 14. A 2 Hertz Pulse Generated by the Fluidic Pulser.

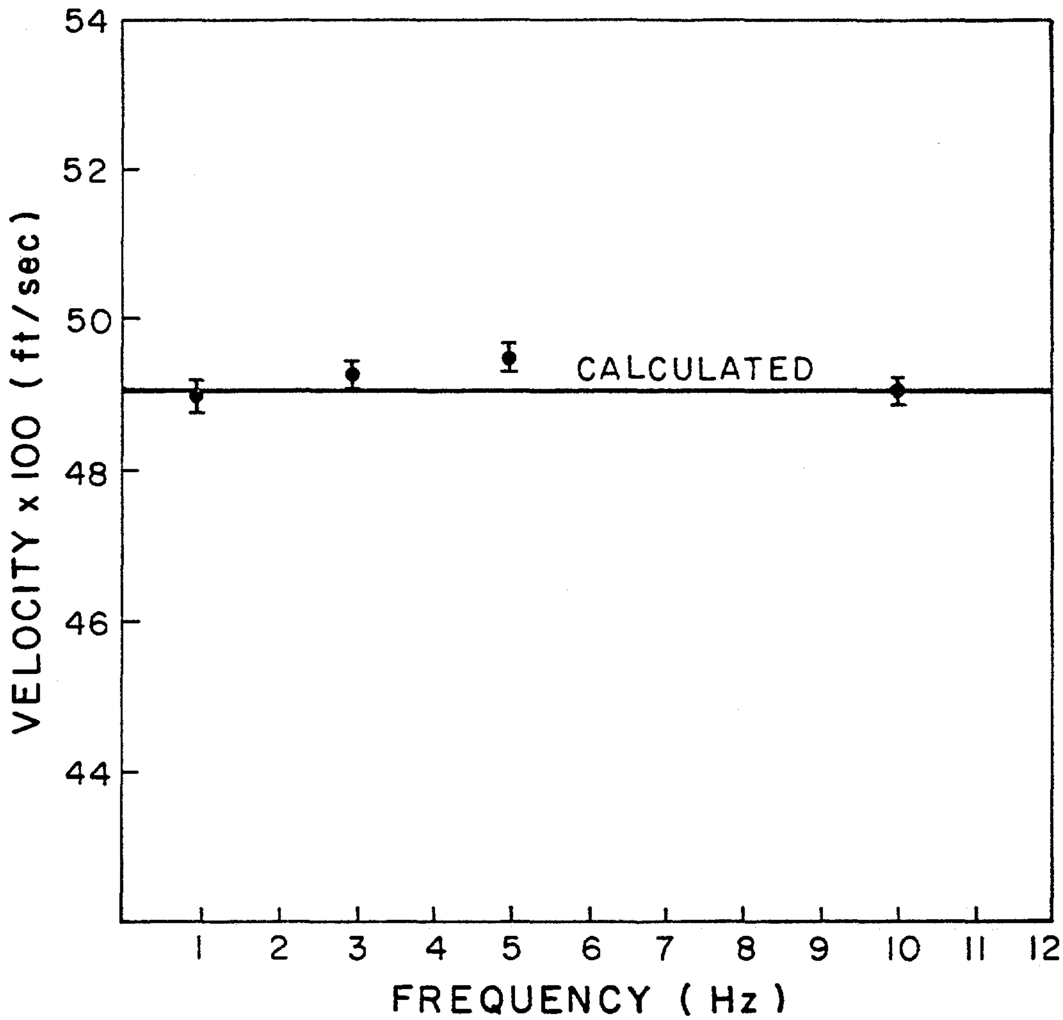

Figure 15. A Plot of the Theoretical and Experimental Velocity Measurements Conducted with Water as the Fluid Medium.

the Fourier transform of the 2 hertz signal in Figure (14). The attenuation is easier to see because it is separated from the noise in the pipe. The attenuation of a wave is not linear but actually an exponential decay. By using the Fourier transform, the intensity (measured in dB) has a logarithmic relationship to the actual magnitude of pulse. Therefore a plot of the intensity versus distance yields a straight line. Figure (17) gives proof of this. By constructing a plot of intensity versus distance for each frequency (figure 17), data was collected to form a plot of attenuation versus frequency at a distance of 9,410 feet. Figure (18) shows the experimental data compared with the straight line values computed by using the attenuation equation derived by Lamb [6]. It can be seen that the data compares well with the theory. It can be noted that an increase in frequency does in fact cause an increase in attenuation or wave decay. Figure (18) also contains data of two other runs made with water. This was the result of air being trapped in the line prior to recording the data.

The air was trapped in the short section of drill pipe which rises to the surface. The impact of this small amount of air on attenuation is very large as can be seen by the upper points in figure (18). A centrifugal pump was used to dipsplace the air from the flow loop. After a period of pumping the tests were repeated.

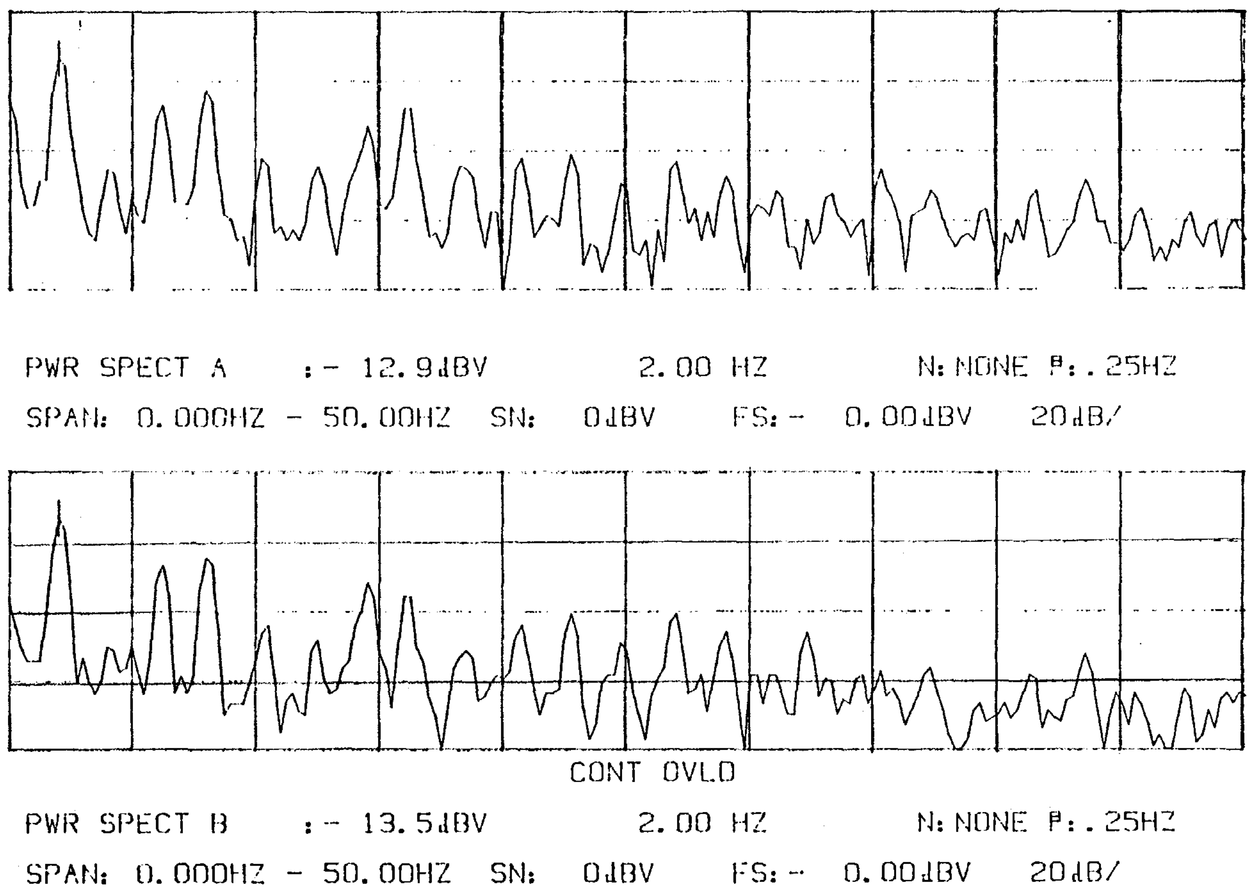

Figure 16. The Fourier Transform of the 2 Hertz Signal in Figure (14). Representative of the Method of Attenuation Measurements.

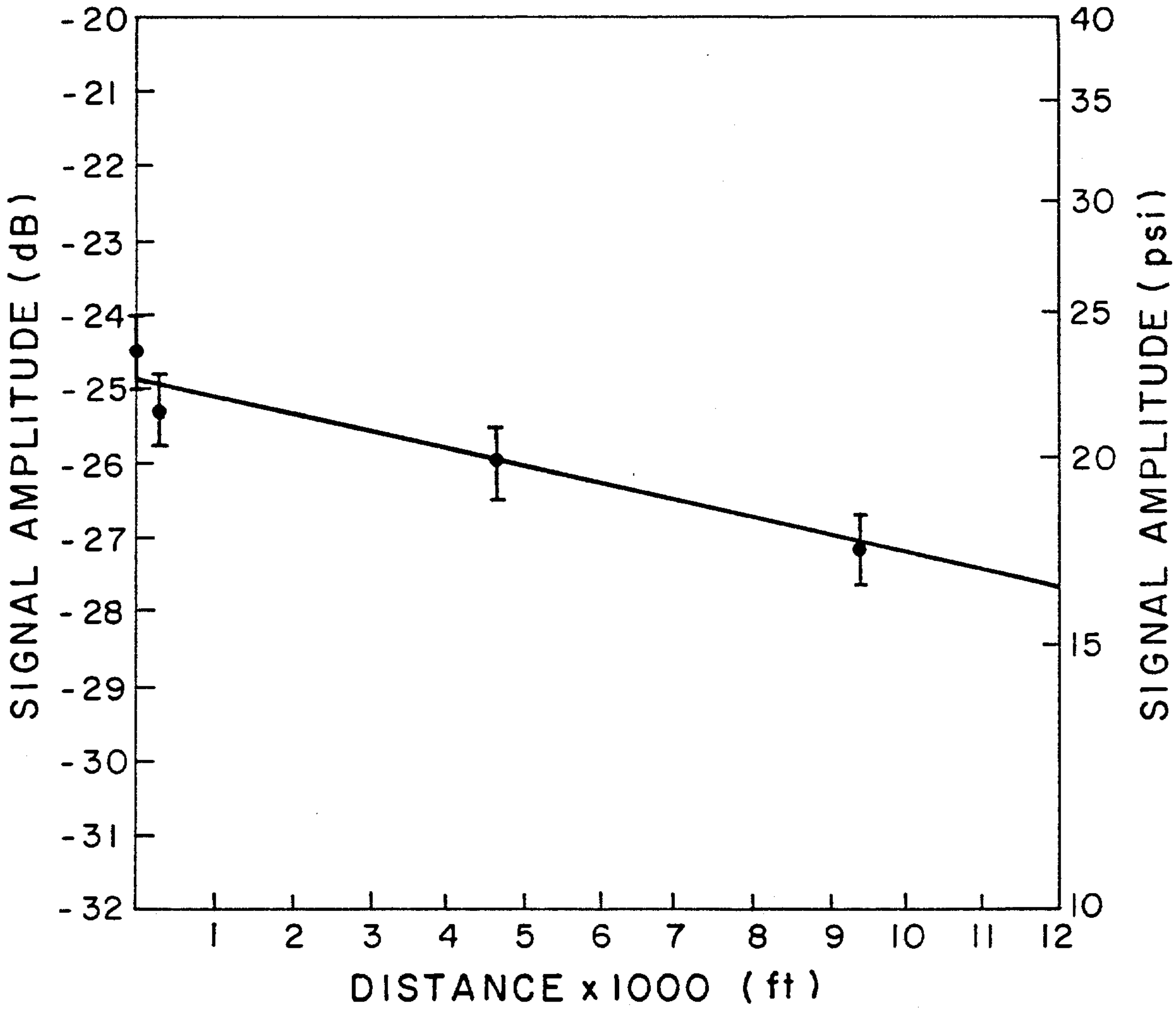

Figure 17. Plot of Signal Amplitude versus Distance of a 3 Hertz Signal in Water.

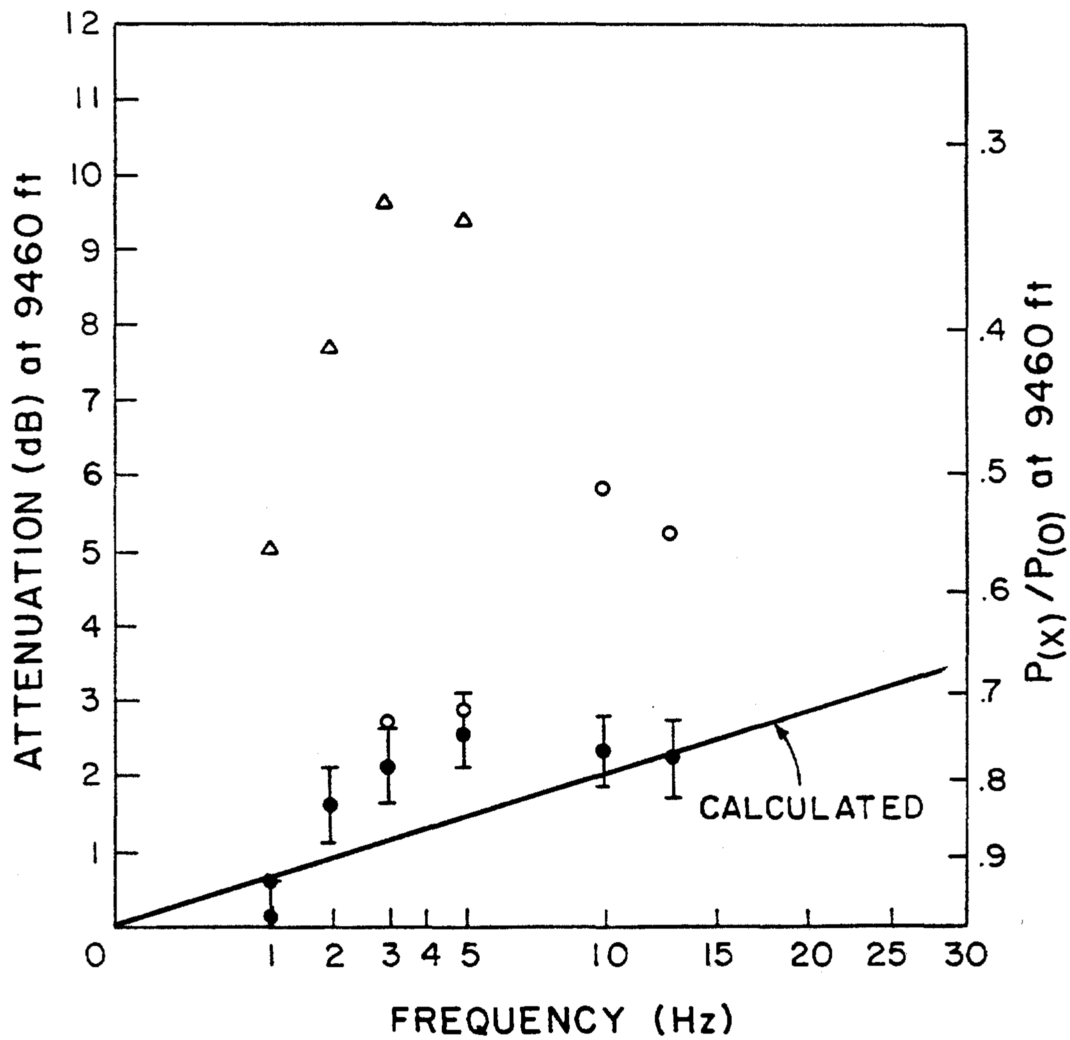

Figure 18. Graph of Resultant Attenuation Data Gathered at Various Frequencies with Water as the Fluid Medium.

The results were a reduced amount of attenuation shown by the circular points in figure (18). As it was clearly indicated that the problem was indeed air entrapment, a complete circulation of the flow loop was executed. In due time the tests were once again repeated and yielded the true attenuation data as shown by the shaded ponts of Figure (18).

4.3 Water-Based Mud

The second fluid used in the experiment was an unweighted water-base mud. The properties of the muds used are listed in table (3). The wave velocities in the mud were determined experimentally and theoretically in the same way as the water experiments. Wave velocity is a function of density and compressibility, therefore a change in wave speed was expected. The compressibility of the mud cannot be found easily in correlations as in the case of water. For theoretical computations of velocity the compressability was computed using the compressabilities of additives and their respective volumes. The measured wave speed was around 4850-4860 feet per second. This was supported by computed velocities of 4853 feet per second (Watters) and 4852 feet per second (White). Figure (19) illustrates how well the theory compares with the data measured in the experiment. The fact that the viscosity varies with the mud does not affect the travel time of the pulse to any noticable extent. This was supported by experimental results and also illustrated in figure (19) by plotting velocity measurements from muds #1, #2, and #3 with viscosities of 14 cp, 20 cp, and 26 cp respectively.

The attenuation of the pulse, however, was greatly affected by viscosity changes. Mud #1 was a low viscosity (14 cp) mud. A significant increase in attenuation was detected by the increase in viscosity. Figure (20) represents the experimental and theoretical plots of frequency versus attenuation for this mud. The experimental data corresponds very closely to the calculated response using the equation by Lamb [6]. Mud #2 which was an unweighted 20 centipoise mud was the second mud used in the experiment. Other properties were held constant as the viscosity was increased. As can be seen in figure (21), the increase in viscosity causes an increase in the slope of the attenuation. To provide furhter proof of this, the viscosity of the flud was increased once again while holding other properties constant (mud #3, 26 cp). Figure (22) shows that once again there is an increase in the amount of attenuation. Throughout the course of this experiment the equations discussed have adequately described the behavior of the pulse. Before the continuation of the tests, there were a couple of changes in the system which will be stated.

The most influential change was the removal of the

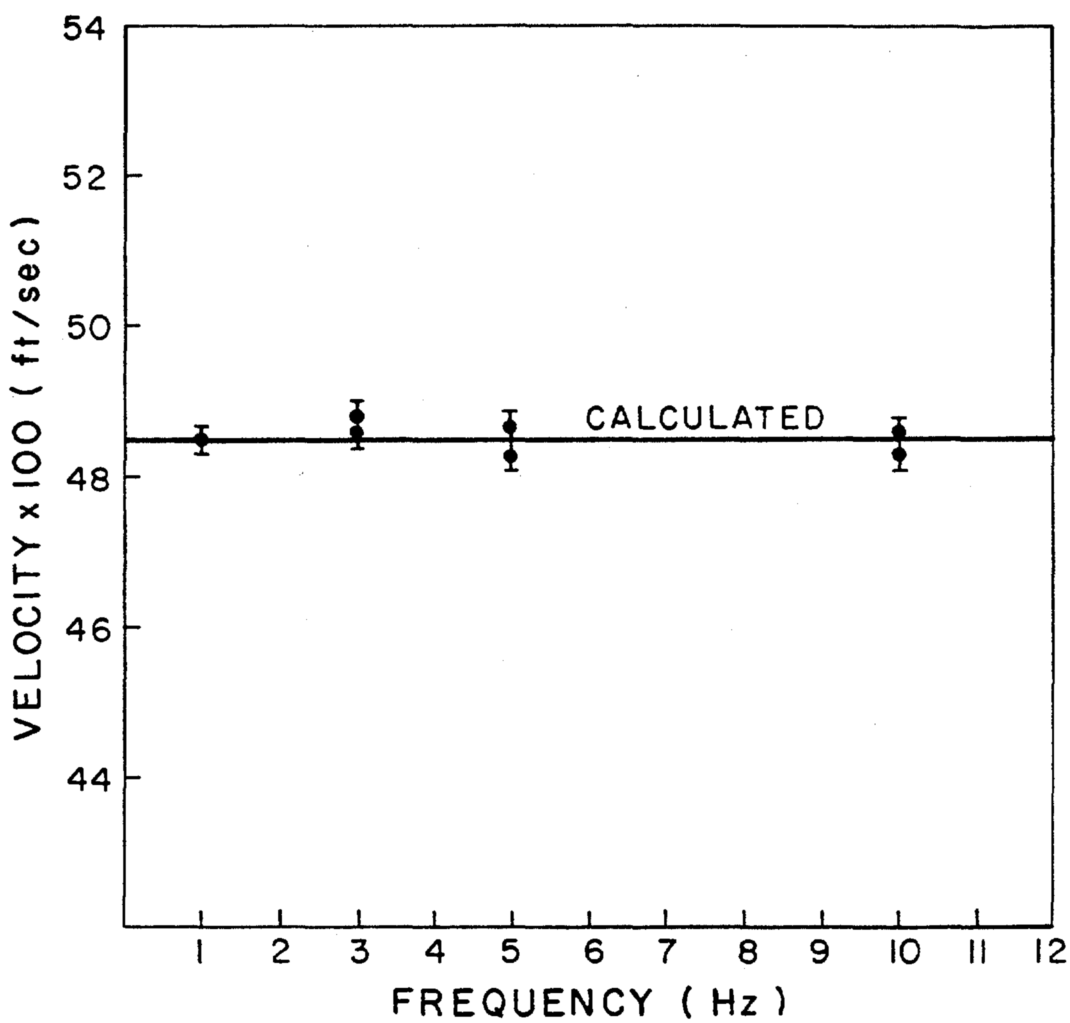

Figure 19. Theoretical and Experimental Velocity Measurements Conducted with Un-Weighted Water-Base Muds of Different Viscosities (Mud #1,#2,#3).

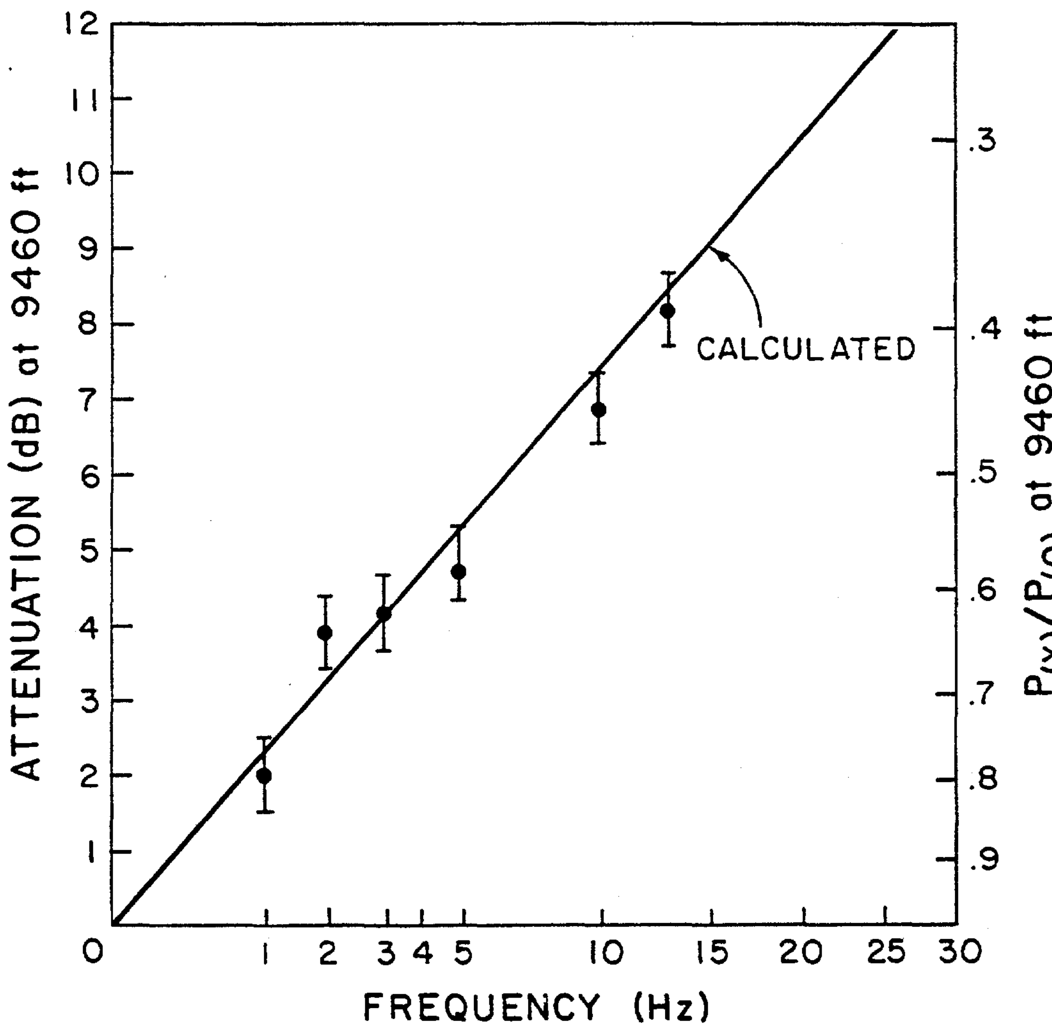

Figure 20. Graph of Attenuation Results Gathered at Various Frequencies with Mud #1 as the Fluid Medium.

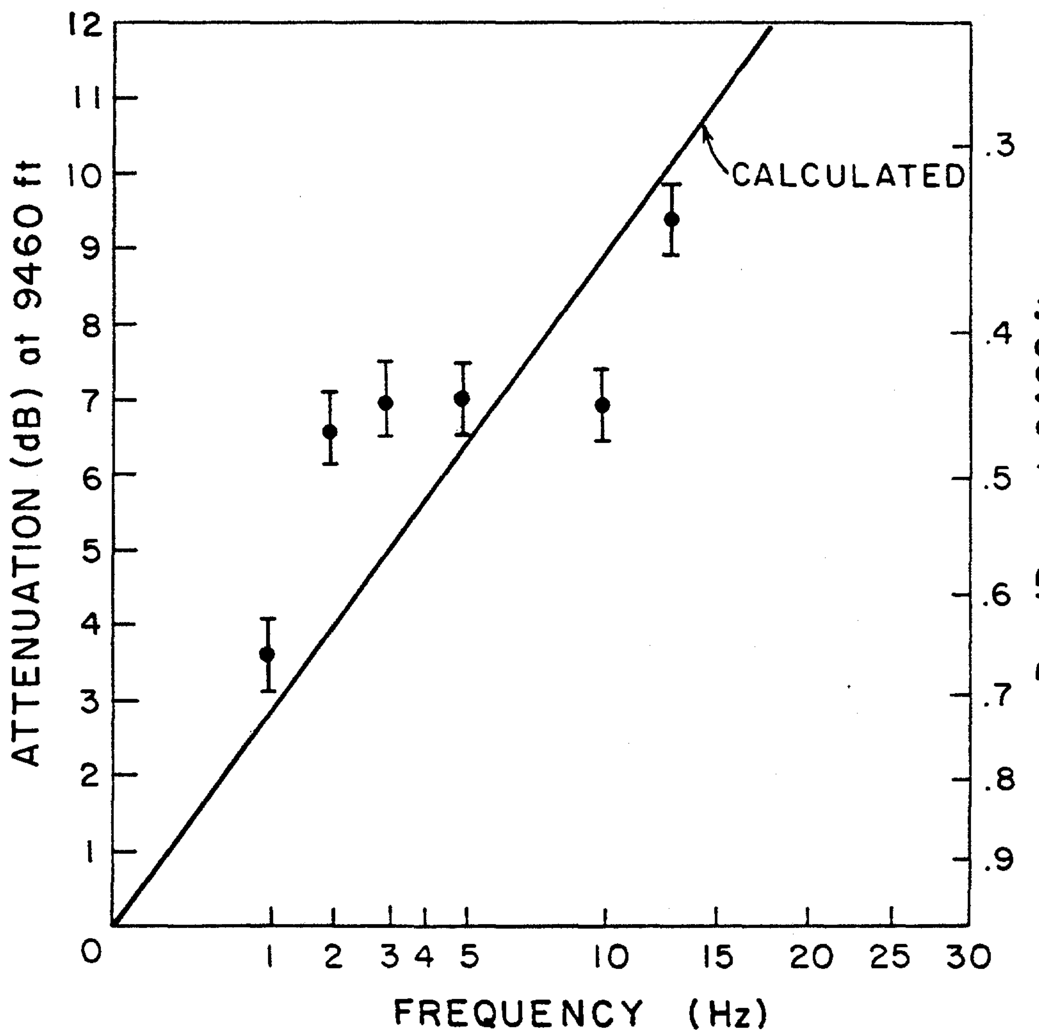

Figure 21. Graph of Attenuation Results Gathered at Various Frequencies with Mud #2 as the Fluid Medium.

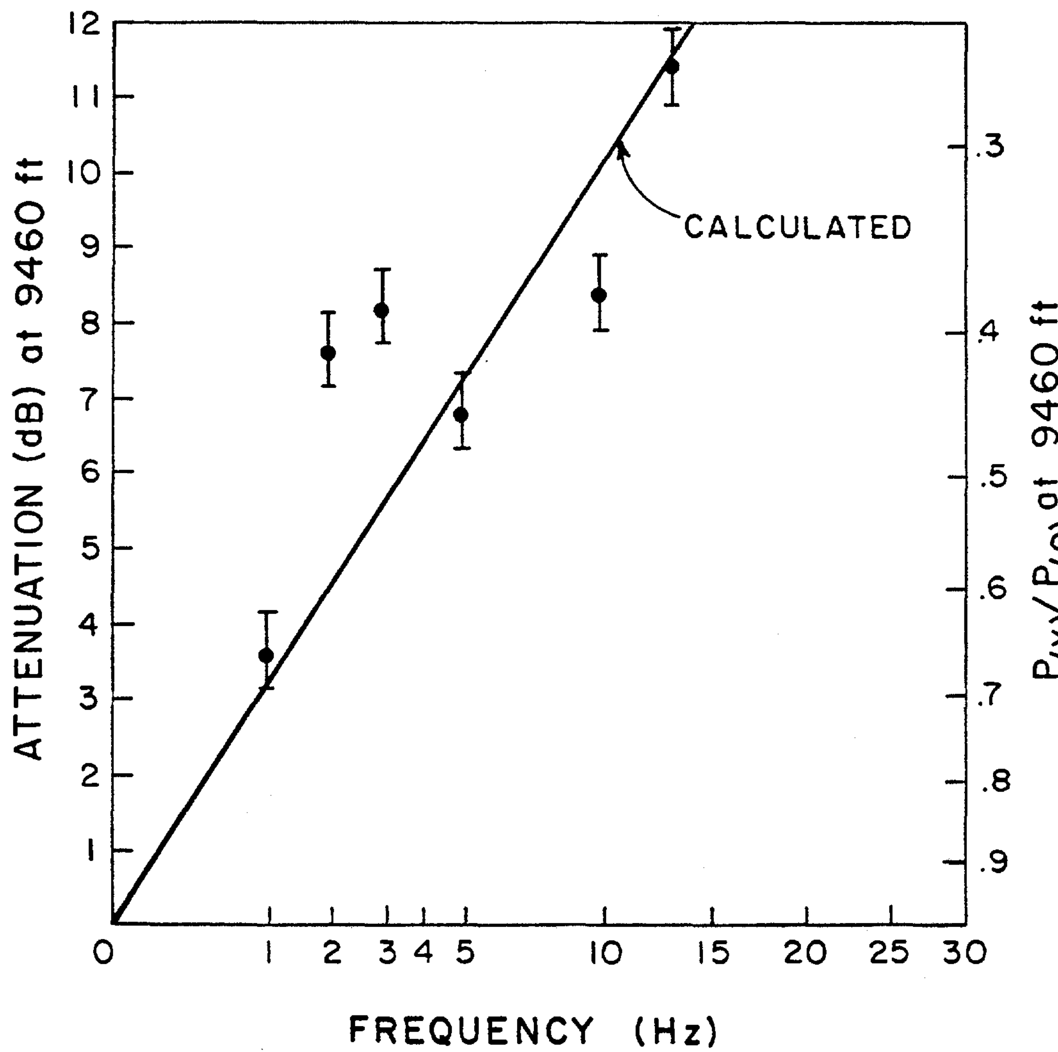

Figure 22. Graph of Attenuation Results Gathered at Various Frequencies with Mud #3 as the Fluid Medium.

2,000 feet storage well as a dampener. This was due to reconstruction work performed on the research center and discontinued access to the well. This resulted in a considerable increase in the amount of pump pulsation. With no other means of dampening the pump noise, there was no choice but to procede with the experiments and work around the effect of the pump. Another modification was brought about from observations made on the first runs. It was noticed that as the frequency was increased the magnitude of the pulse at the pulser decreased. There was no theoretical explanation for this except that the pulser was not operating efficiently. After considering the system it was determined that the line impedance for the 300 feet of electrical wire was preventing the 24 volt power supply from reaching the solenoid operated valve. As a result the power supply was stepped up to 30 volts. The effect on signal amplitude was enormous. The signal increased by 100 per cent at 1 hertz. The signal still decreased as frequency was increased but a variable voltage supply was not available to further examine its effect on the pulser.

4.4 Oil-Base Mud

Following the innovations in the system the experiments were continued with an oil-base mud. This mud consisted of a 84/16 oil-water ratio. It also was an unweighted mud of 8.5 pounds per gallon. Other properties of the oil-base mud are stated in table (3) under mud #4. With the pulser operating with an improved efficiency, much better data was obtained. Although the signals were distorted with noise, frequencies as high as 25 hertz were reached and analyzed. Figure (23) is an example of a 13 hertz signal generated by the pulser. The signal appears clear in figure (23) due to the fact that a great deal of the pump noise, which measured close to 60 psi at the pump, had attenuated out.

The velocity measurments were measured using transparent overlays as in the previous cases. The velocity was experimentally measured to be 4545-4553 feet per second. This again compared well with the calculated data a shown in figure (24). The calculated velocity was 4550 feet per second using the equation by Watters [3]. The computations using the equation by White [4] were again very close to that of Watters with 4548 feet per second. The velocity equations appear to be a valid means of evaluating pressure wave velocities in drill pipe containing a fluid of known density and compressibility.

The attenuation as before was computed for each frequency. Figure (25) shows that the pressure pulses are much stronger than that previously shown in figure (17). Figure (25) also shows that the pulse still maintains an exponential decline as it travels over a distance. The

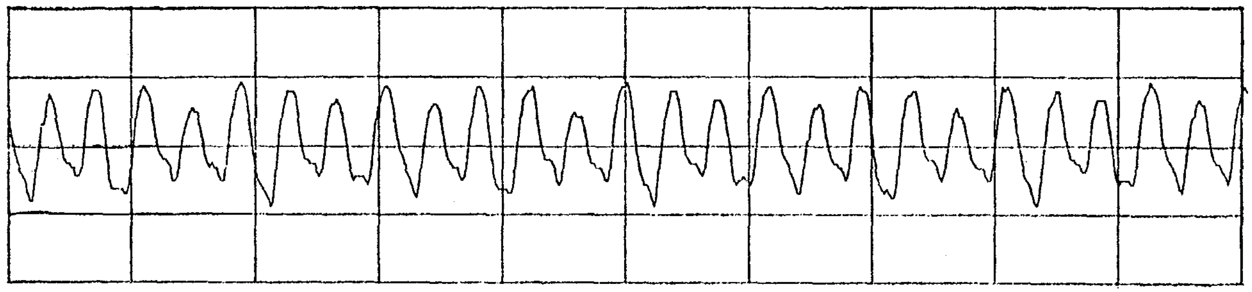

TIME A: 2.1E-01V 1.99SEC 200.00mSEC/

SPAN: 0.000HZ -100.00HZ SN: 3.6-01V FS: ±5.0-01V 2.5-01V/

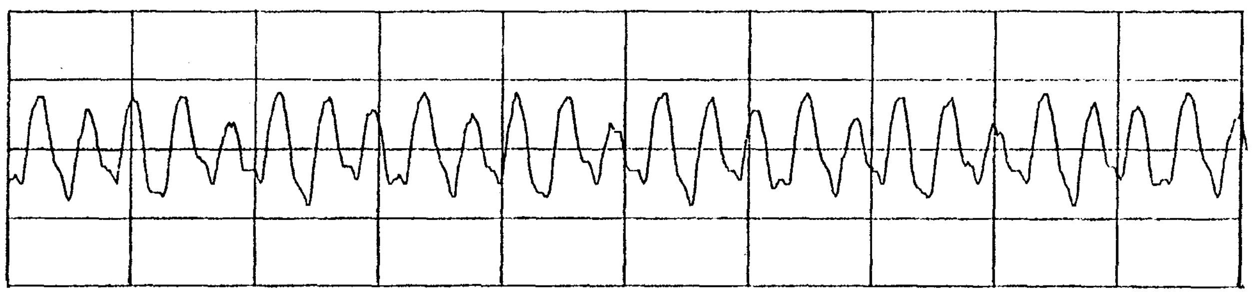

TIME B: 9.4E-02V 1.99SEC 200.00mSEC/

SPAN: 0.000HZ -100.00HZ SN: 3.6-01V FS: ±5.0-01V 2.5-01V/

Figure 23. A 13 Hertz Pulse Generated by the Fluidic Pulser.

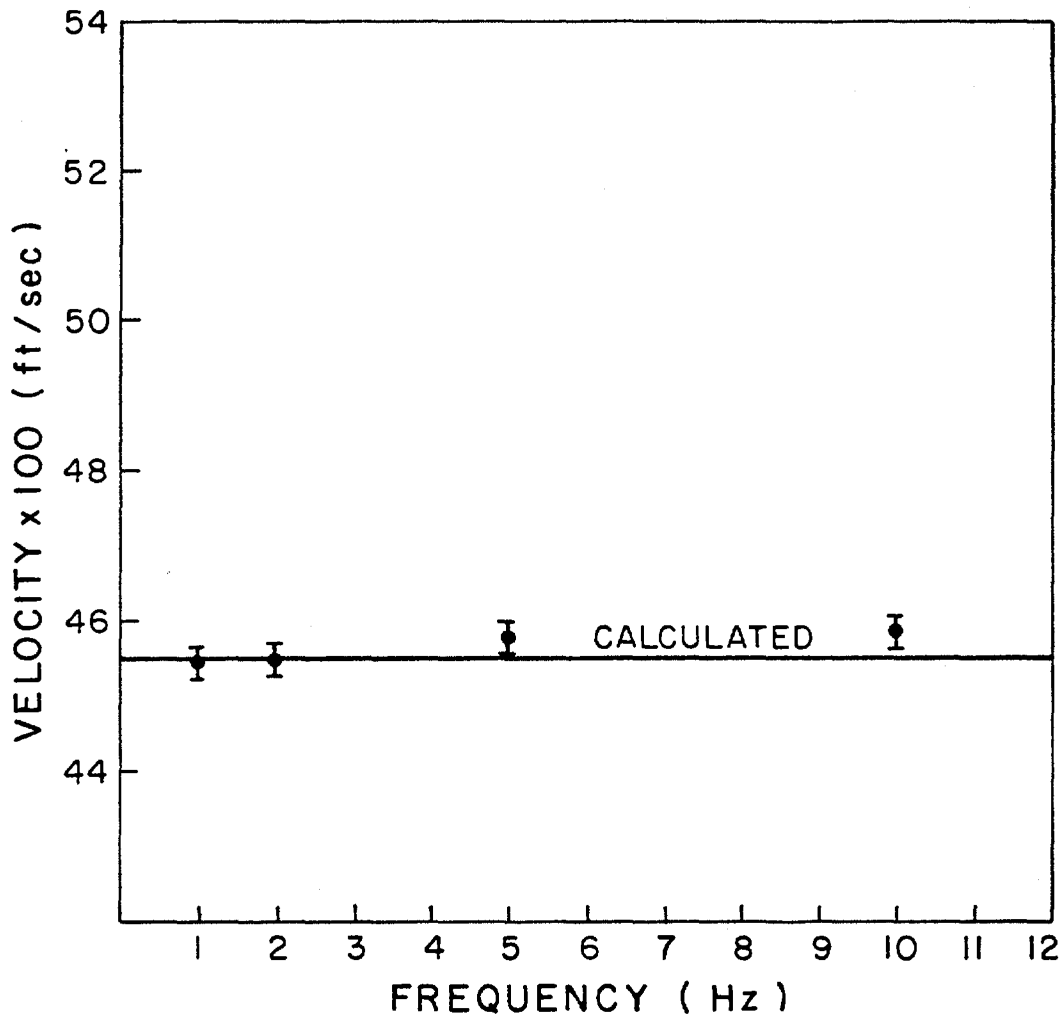

Figure 24. Theoretical and Experimental Velocity Measurements Conducted with an Un-Weighted Oil-Base Mud (Mud #4).

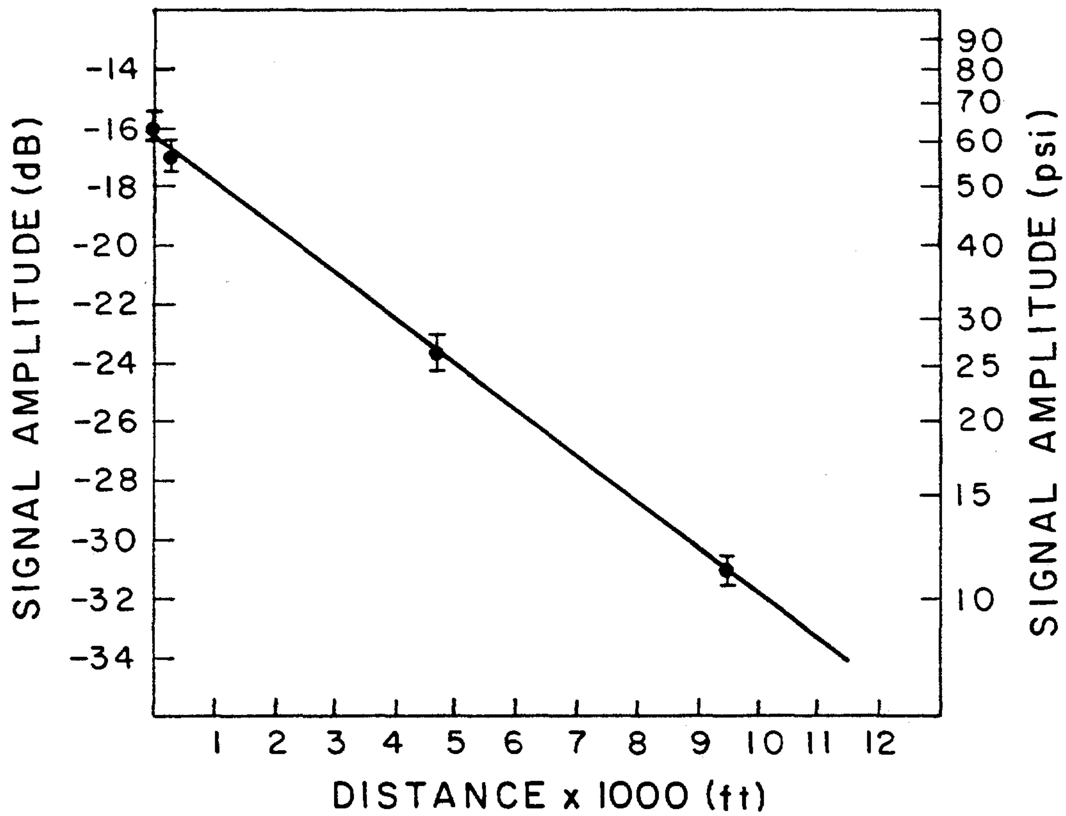

Figure 25. Plot of Signal Amplitude Versus Distance for a 13 Hertz Signal with Oil-Base Mud (Mud #4) as the Fluid Medium.

amount of attenuation was measured and plotted versus frequency in figure (26). Although the attenuation was much greater when the oil-base mud was the fluid medium, the experimental data remained very close to the calcu lated trend using the equations by Lamb [6]. The experiment was concluded with the usual calibration check following a run. The equipment checked out very well and supported the accuracy of the data collected.

4.5 Discussion

The data collected during the course of the experiment appears to be of good quality. The velocity measurements correlate well with the theory of White and Watters. The error bars were included in the plots of the experimental data because of human error in the measurement. The method of velocity measurement was repeated using the same data. The difference between between the two measurements of velocity was used as an indication of error. The time differences measured from one transducer to another were less than a second and measured in milliseconds. The influence of 10 to 20 milliseconds over a few thousand feet reflects the indicated error. The difference of the measured and calculated velocities amounted to less than 1 percent. With this accuracy one can safely use the theory derived by White and Watters to predict pressure wave velocities in drill pipe.

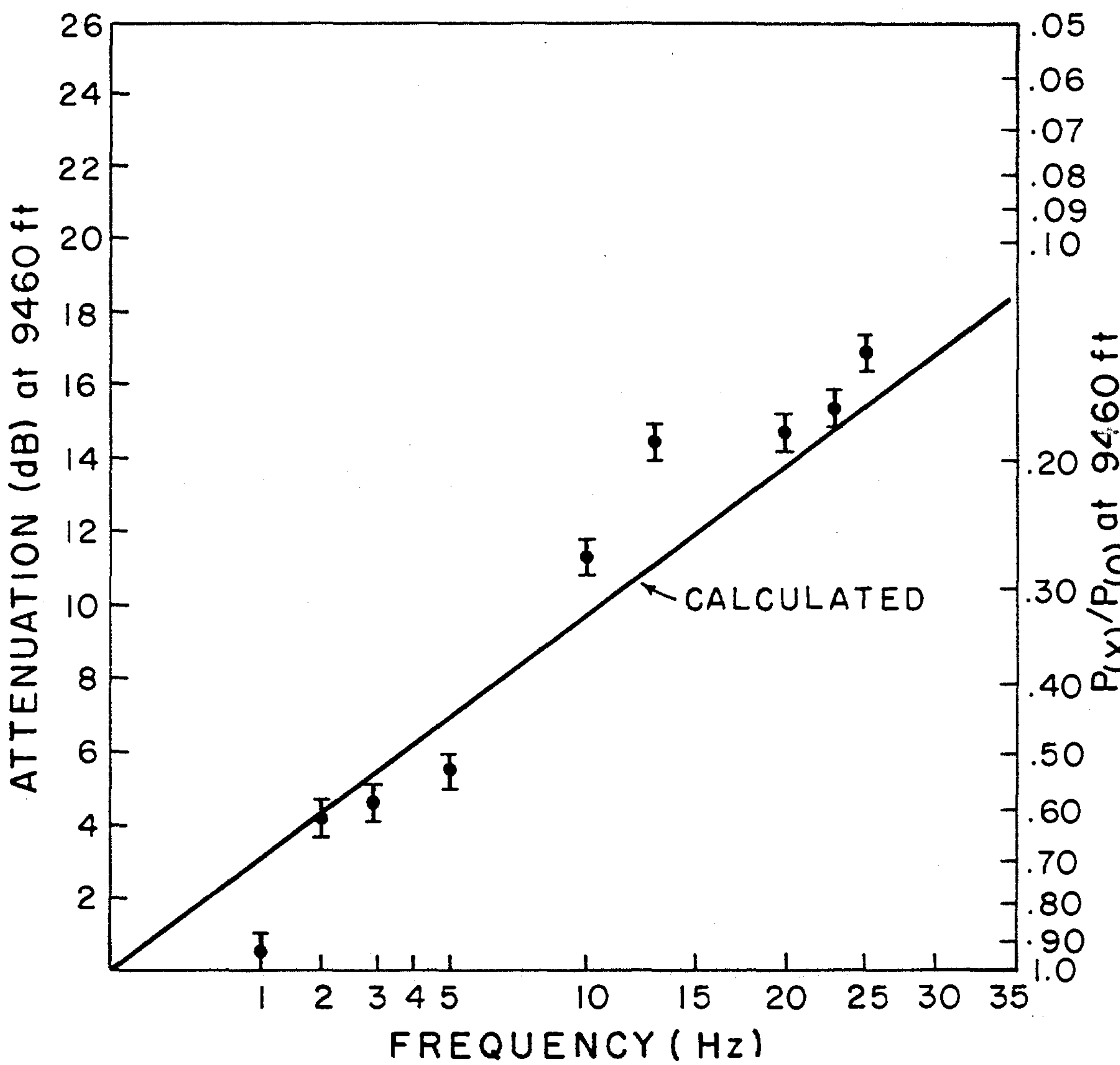

Figure 26. Graph of Attenuation Results Gathered at Various Frequencies with Mud #4 as the Fluid Medium.

The attenuation data however, followed the trend of the theory by Lamb, but showed slight scattering as the viscosity was increased. This could possible be a result of one or a combination of pump noise effects and the fact that the equations were derived for a Newtonian fluid. As the plastic viscosity is increased the fluid would tend to go further from a Newtonian towards a Bingham Plastic state. Although one would expect some deviation of experimental data from theoretical data, a closer correlation would be expected if further research was performed with the use of a couple of 5 to 10 gallon bladder type pulsation dampeners.

By properly charging the dampeners (approximately 60 percent of pump pressure) a very large amount of the pump noise can be eliminated. Such an improvement could make a significant difference in the results of the pulse propagation tests.

CHAPTER 5

CONCLUSIONS AND RECOMMENDATIONS

5.1 Conclusions:

1) The velocity of a pressure pulse in drill pipe has been studied and found to be dependent on the density and compressibility of the fluid medium.

2) The equations by White [3] and Watters [4] have been proven to predict the pressure wave velocities very accurately. Properties that must be known to use these equations are:

Pipe – Young's Modulus, Outside diameter,
Inside diameter, and Poisson's ratio.

Fluid – Compressibility and density.

3) The fluidic mud pulser used in the experiment has proven to produce detectable pulses up to 10,000 feet away and at frequencies as high as 25 hertz.

4) Pressure wave attenuation was analyzed and indeed found to be of an exponential decay over distance.

5) Attenuation of a pulse was also found to be very sensitive to viscosity, compressibility, and frequency at which the pulse was transmitted.

6) The equations by Lamb [6] on this subject were supported by experimental data and found to be useful in describing pulse functions similar to those used in MWD systems.

7) It was also discovered that very small volumes of gas could have a detrimental effect on the attenuation of a wave. This could come into effect when air is trapped in the drillstring while making connections during standard drilling operations. Directional data is often transmitted to the surface following a connection.

5.2 Recommendations

1) It is part of the projected research that a heavy weight mud be used in similar tests to confirm the effect of density on velocity and wave attenuation. Pulsation dampeners are also to be included in these experiments to reduce the effect of the pump on the signals generated by the pulser.

2) The use of a micro-computer to transmit coded signals is recommended as part of the future research. It has been proven that signals can be detected at higher frequencies than in present use. It would be of further interest to determine if it is possible to encode data at the higher frequencies through the use of the popular binary coding system. This would offer proof that data could be transmitted at higher frequencies and possibly lead to further field testing of mud pulsers.

REFERENCES

1. Andrew Roberts, Robert Newton, Frederick Stone: "MWD Field Use and Results in the Gulf of Mexico," Teleco Oilfield Services Ltd., SPE 11226 57th Annual Fall Technical Conference, September, 1982.

2. Marvin Gearhart, Kelly A. Ziemer, Orien Monroe Knight: "LMud Pulse MWD (Measurement-While-Drilling) Systems Report," Gearhart Industries, SPE 10053 56th Annual Fall Technical Conference, October, 1981.

3. Gary Z. Watters, Modern Analysis and Control of Unsteady Flow in Pipelines, Ann Arbor Science, Ann Arbor Michigan, pp 29-39, 1980.

4. James Edward White, Seismic Waves: Radiation, Transmission and Attenuation, Marathon Oil Co., McGraw Hill, pp 148-158, 1965.

5. E. L. Holmboe, W. T. Rouleau, "The Effect of Viscous Shear on Transients in Liquid Lines," Carnegie Institute of Technology, Paper No. 66-WA/FE-11, 1966.

6. Horace Lamb, Hydrodynamics, Dover, New York, NY, 1945.

7. Aurthor T. Ippen, Marks Mechanical Engineers' Handbook, McGraw Hill, New York, 1951.

8. "Halliburton Cementing Tables", Halliburton Services, 1981.

9. "Le Forage aujourd'hui" (Drilling Today) Vol.2, Technip Editions, Paris, 1970.

10. B. J. Patton, W. Gravely, J. K. Godbey, J. H. Sexton, D. E. Hawk, V. R. Slover, J. N. Harrell, "Development and Successful Testing of a Continuous-wave Logging-While-Drilling Telemetry System," Mobil Research and Development Corp., Journal of Petroleum Technology, pp. 1215-1221, October, 1977.

11. "Quartz Sensors," PCB Piezotronics, Inc., 1984.

12. Allen B. Holmes, "The Fluidic Approach to Mud Pulser Valve Design for Measurement-While-Drilling Systems," HDL Technical Report, U.S. Army, October 4, 1984.

13. Allen B. Holmes, "Fluidic Mud Pulse Telemetry," Harry Diamond Laboratories, U.S. Army, 1983.

14. "Operating Manual Model 5820A Cross Channel Spectrum Analyses," Wavetek Rockland, Inc., 2nd Edition, 1983.

15. Paul A. Tipler, "Harmonic Analysis and Synthesis," Tipler Physics, Worth Publishers, Inc., New York, pp. 552-56, 1976.

16. Erwin Kreyszig, "Fourier Series and Integrals," Advanced Engineering Mathematics, John Wiley & Sons, New York, Fourth Edition, pp. 468-508, 1979.

17. Milton B. Dobrin, "Enhancement of Seismic Reflection Data in Processing Centers," Introduction to Geophysical Prospecting, McGraw Hill, Third Edition, pp. 157-165, 1976.

18. J. W. Codez, P. A. W. Lewis, P. D. Welch, "The Fast Fourier Transform Algorithm: Programming Considerations in the Calculation of Sine, Cosine, and Laplace Transforms," IBM Corp., August 22, 1969.

VITA

Joseph Alan Carter was born the third son of Billy and Jean Carter on November 26, 1961, in Hattiesburg, Mississippi. He attended Runnelstown High School in the rural outskirts of Hattiesburg. Upon graduation in May of 1979, he spent one year at Jones County Junior College in pre-engineering. In 1980 Joseph enrolled at Mississippi State University where he obtained a Bachelor degree in Petroleum Engineering. While at M.S.U. he was an officer of the student chapter of the Society of Petroleum Engineers and Pi Epsilon Tau. In May of 1983, he graduated from M.S.U. and took employment with Services, Equipment, and Engineering. In the Fall of 1984, he applied and was accepted into graduate school at the Louisiana State University to persue a Master of Science degree in Petroleum Engineering.